Food and Bioprocess Technology (2026) 19:168
https://doi.org/10.1007/s11947-026-04259-4

RESEARCH

Proof-of-Concept for Cell Culture-Based Duck Fat Production on a Laboratory Scale

Andy Díaz-Maneh[1,2] · Andreu Camacho-Sucarrats[2] · Javier Fuenmayor[2] · Natasa Ilic[2] · Natalia García-Aranda[2] · Yuliana Enciso[2] · Mario Notari[2] · Francesc Gòdia[1] · Jesús Lavado-García[3] · Raquel Revilla-Sánchez[2]

Received: 21 June 2025 / Accepted: 2 February 2026

Abstract

Cultured meat has been gaining ground in recent years as an innovative approach to address the potential scarcity of meat supply. Fat is one of the key components of meat in terms of flavor and juiciness. However, the production and scale-up of fat from agriculturally relevant animals have not been extensively investigated, particularly in scalable bioreactor systems. The culture of primary duck embryonic fibroblast (DEF) proliferation and adipogenesis in various lab-scale bioreactors for cultured meat purposes was explored. Cytodex 1 microcarriers were used to culture DEF in two proprietary serum-free media: ProDuck4.0 for proliferation and LipoDuck2.0 for adipogenesis. Proliferation and differentiation conditions of DEF were optimized in shake flasks through Design of Experiments (DoE) and then the culture was transferred to lab-scale bioreactors operating in perfusion with different agitation regimes. A rocking motion bioreactor (RMB), an orbitally shaken bioreactor (OSB), and a stirred tank bioreactor (STB) were assessed to scale up the production process. Results showed that DEFs exhibited high sensitivity to shear stress, particularly in RMB and OSB systems, which led to impaired cell growth. In contrast, STB supported DEF proliferation and adipogenic differentiation, reaching full confluency and a cell concentration of 489,000 cells·mL^{-1} and an intracellular triglyceride accumulation of 380 pg·cell^{-1}, comparable to those achieved in shake flasks. These findings highlight the potential of using STBs for scaling up duck fat production for cultured meat applications.

Keywords Cultured meat · Adipose tissue · Microcarrier · Bioreactor · Design of experiments

Introduction

The global population has doubled in the last five decades, leading to a substantial increase in the demand for food products, and global demand for food products is projected to continue rising in the coming years. Among the most impacted will be animal-derived products such as meat and dairy, which are expected to experience a substantial surge in demand (Sands et al., 2023). It is estimated that this rise in global population will escalate meat consumption by 47.9 million tons over the next decade (OECD Publishing, 2025; Ritchie et al., 2023).

Several technological solutions have been proposed to address the issue of food scarcity (Andreani et al., 2023; Smetana et al., 2015). Among them, cellular agriculture represents an emerging technological approach under active development that has seen increasing research activity and commercial interest in recent years, especially regarding its most popular product: cultured meat (Eibl et al., 2021).

Meat is mainly composed of muscular, connective, and fat tissues, with fat being a key contributor to sensory properties such as flavor, juiciness, and texture (Shin et al., 2023; Valsta et al., 2005). The lipid composition of fat varies depending on the source tissue and species (Pereira & Vicente, 2013; Valsta et al., 2005). In recent years, several studies have demonstrated that adipose tissue can be generated in vitro

✉ Andy Díaz-Maneh
diazmanehandy@gmail.com; andy.diaz@autonoma.cat

1 Grup d'Enginyeria de Bioprocessos I Biocatàlisi Aplicada, Escola d'Enginyeria, Universitat Autònoma de Barcelona, Campus de Bellaterra, Cerdanyola del Vallès, 08193 Barcelona, Spain

2 CUBIQ FOODS S.L., Carrer Palautordera 24, 08401 Granollers, Barcelona, Spain

3 Novo Nordisk Foundation Center for Biosustainability, Technical University of Denmark, 2800 Kgs. Lyngby, Denmark

Published online: 16 February 2026

from relevant animal cell types. Bovine fibro-adipogenic progenitors have been differentiated into mature adipocytes forming three-dimensional adipose tissue (Dohmen et al., 2022), and engineered constructs based on bovine preadipocytes embedded in alginate matrices have reproduced the marbling patterns characteristic of conventional meat (Zagury et al., 2022). More recently, bovine adipose-derived stem cell spheroids have been dynamically cultured and differentiated as to produce bovine fat (Klatt et al., 2024). In addition to agriculturally relevant species, researchers have explored the potential of producing fat from non-traditional sources, such as the insect species *Manduca sexta* (Letcher et al., 2022).

Research has also been conducted on other agriculturally relevant species like chickens (Pasitka et al., 2023). In this study, the immortalized chicken fibroblasts were cultivated in suspension at hich cell densities using a perfusion approach, reaching $108 \cdot 10^6$ cells/mL. Also, the immortalized fibroblasts were differentiated into adipocyte-like cells using soy lecithin as an adipogenesis inductor, showing an increased expression of key adipogenic markers such as FABP4 and PPARγ. When incorporated into plant-based matrices, this cultured fat supplied the aroma and flavor attributes characteristic of chicken, enabling hybrid products with sensory profiles closer to conventional meat.

Most research conducted in academic institutions has focused on producing cow- and pig-cultured meat derivatives (Yun et al., 2024). To the best of our knowledge, no studies have been conducted so far using duck cells for cultured meat purposes, with few companies working with duck cells and no commercially available products on the market (Yun et al., 2024).

Despite its potential, cultured fat faces several challenges, the most pressing of which is whether it will be possible to produce biomass at scale at a competitive cost using this technological approach (Yun et al., 2024). To this end, the production of large quantities of cells in large-scale bioreactors would be required. The culture of high concentrations of cells in bioreactors has been extensively studied and is widely used in the biomanufacturing industry, with scales reaching up to 30,000 L bioreactors, particularly for Chinese hamster ovary (CHO) cell cultivations (Sharma et al., 2022). However, the scale-up and intensification processes necessary to reach such scales presents engineering challenges, especially for novel cell lines derived from agriculturally relevant species, since their biology and characteristics have been less studied compared to others conventionally used in biomanufacturing (Fish et al., 2020; Yun et al., 2024).

The cultivation of animal cells in large-scale bioreactors is essential for various biomanufacturing applications, with rocking motion bioreactors (RMB), stirred tank bioreactors (STB), and orbitally shaken bioreactors (OSB) being common bioreactor types (Sharma et al., 2022). RMBs are operationally simple and require minimal setup but are limited in scalability, reaching up to 200 L (Sharma et al., 2022). STBs, widely used in the biopharmaceutical industry, can scale up to 30,000 L, making them suitable for producing therapeutic proteins and vaccines (Fang et al., 2022; Nelson, 2024; Sharma et al., 2022). OSBs of 5L have shown similar yields to that of 3L STBs regarding cell growth, antibody yield and quality (Monteil et al., 2016). Each bioreactor type presents trade-offs in scalability, mixing efficiency, and operational complexity, and selection depends on culture volume, cell type sensitivity, and oxygen transfer requirements.

The cell line itself is one of the key determinants in the final configuration of the bioproduction process (Shaikh et al., 2021). From a biomanufacturing perspective, cell lines can be divided into two categories based on their ability to grow in suspension or not (Demirden et al., 2024). Most animal cells are anchorage-dependent, meaning they must attach to a surface to grow and proliferate. These connections are crucial, not only for their proliferation but also for preventing senescence or programmed cell death (Reddig & Juliano, 2005). Because of the many advantages that suspension cell cultures provide, many naturally anchorage-dependent cell lines have been adapted to grow in suspension (Demirden et al., 2024; Fang et al., 2022). This adaptation often involves a prolonged phase of selection, where cells that can proliferate in suspension are selected over multiple passages, sometimes exceeding 10 passages (> 30 days in culture) (Couto et al., 2024). This process is challenging and may not be feasible for primary cell lines, leading to the development of several strategies to cultivate anchorage-dependent cells on relatively large scales (Thomassen et al., 2012). These include roller bottles and fixed-bed bioreactors, and conventional bioreactors combined with cell spheroids/aggregates or scaffolds such as microcarriers (Bellani et al., 2020; Klatt et al., 2024; Kulus et al., 2023). A central challenge common to these strategies is the sensitivity of cells to culture conditions, especially regarding shear stress (Julaey et al., 2016).

Microcarriers are small bioactive beads to which anchorage-dependent cells can attach and proliferate (Bodiou et al., 2020). They have been used in the manufacturing industry since the 1980 s, with renewed interest due to the rise of applications requiring adherent cell cultures, such as cell therapies and cellular agriculture (Bellani et al., 2020; Bodiou et al., 2020). Microcarriers can be classified as microporous and macroporous. Macroporous microcarriers offer increased surface area and protection against shear stress. Microporous microcarriers provide a surface only on their outer layer, exposing cells to mechanical stress but facilitating enzymatic action and cell recovery (Koh et al., 2020; Panchalingam et al., 2015; Rodrigues et al., 2013). Most commercially available microcarriers face challenges

in cultured meat production: they are often expensive or unsuitable for food applications, and the research on their use with non-conventional animal cell lines is still scarce (Bodiou et al., 2020). On the other hand, these microcarriers provide a good model for process development purposes while researchers develop new edible microcarriers. An example of this is the Cytodex 1 microcarriers. They are composed of dextran functionalized with N, N-Diethyl aminoethyl (DEAE) groups, which make them unsuitable for food production, and are only going to be used in this work for process development purposes (Pörtner, 2007).

Although some studies have addressed the cultivation of duck cells in bioreactors, these were primarily directed toward vaccine and biopharmaceutical production using suspension-adapted genetically modified duck cell lines (Fu et al., 2012; Lohr et al., 2014; Madeline et al., 2015; Nikolay et al., 2018), with no studies addressing scale-up for applications in cultured meat. In particular, while cultured fat has been reported for bovine and porcine cells, it has not yet been described for duck, a species of high gastronomic relevance. The aim of this work is to develop and optimize protocols for the proliferation and adipogenesis of fibroblasts obtained from an agriculturally relevant animal such as the duck, and to evaluate their performance across different lab-scale bioreactors for cultured duck fat production.

Materials and Methods

Isolation of the Duck Embryonic Fibroblasts (DEF) from Fertilized Eggs

Primary DEF were isolated from Khaki Campbell fertilized eggs following a three-step procedure (schematized in Fig. 1): (1) preparation of culture medium, enzymatic solution, and sterile tools, (2) embryo extraction, and (3) DEF dissociation.

Briefly, fertilized eggs were incubated for 8 days at 38 °C, disinfected with ethanol, and opened under a biosafety cabinet. Embryos were excised, non-target tissues removed, and the central portion finely minced. Tissue fragments were digested with 0.25% trypsin–EDTA at 37 °C for 10 min, the reaction was stopped with serum-supplemented medium, and the suspension filtered through 70–40 µm cell strainers to obtain a single cell solution. Cells were pelleted by centrifugation, resuspended, and seeded at 3×10^4 cells·cm^{-2} in culture flasks. Detailed protocols for medium preparation, tool sterilization, and embryo handling are provided in Supplementary Material.

Cell Culture Media and Culture Conditions

Dulbecco's Modified Eagle Medium: Ham's F-12 Nutrient Mix (1:1)

A modified version of Dulbecco's Modified Eagle Medium: Ham's F-12 mix 1:1 (DMEM/F-12) without L-glutamine, D-glucose and sodium bicarbonate was obtained from Cytiva (Ref. SH31036.02, Cytiva, Washington D.C., USA). Medium powder was weighted and dissolved using distilled water at a final concentration of 8.48 g·L^{-1}, together with 3.151 g·L^{-1} of glucose (Ref. G7021, MilliporeSigma) and 2.438 g·L^{-1} of sodium bicarbonate (Ref. SO0131005P, Scharlab S.L., Sentmenat, Spain) using a magnetic stirrer and was then subjected to filter sterilization using a 0.22 mm Stericup (Ref. S2GPU02RE, MilliporeSigma). The mixture, referred from now on as basal medium, was stored at 4 °C until further use.

Preparation of Non-essential Amino Acid Solution

Minimal essential medium (MEM) non-essential amino acid (NEAA) concentrate was formulated 100X by dissolving glycine, L-alanine, L-asparagine·H2O, L-aspartic acid, L-glutamic acid, L-proline, and L-serine in distilled water. A magnetic stirrer was used to achieve a homogenous solution, which was then sterilized by filtration using a 0.22 mm Stericup (Ref. S2GPU11RE, MilliporeSigma) and stored at 4 °C until future use. See concentrations in Table S1 in the Supplementary Material.

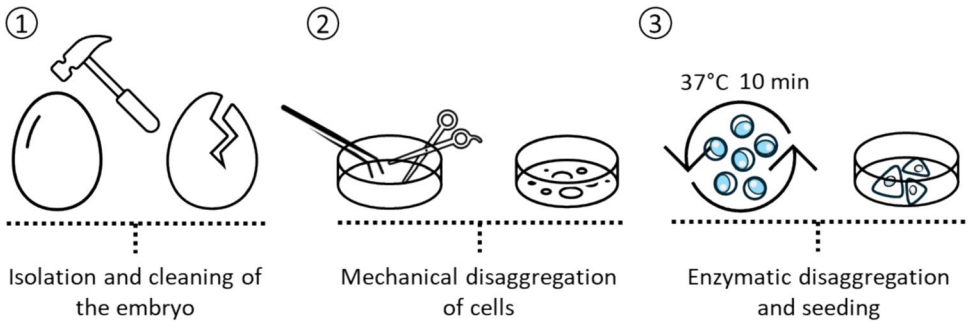

Fig. 1 Schematic representation of the isolation of duck embryonic fibroblasts from Khaki Campbell fertilized eggs

Preparation of Serum-Supplemented Media

Culture medium for DEF was prepared by supplementing DMEM/F-12 with 1% NEAA, 1% Penicillin–Streptomycin ($P{\cdot}s^{-1}$) (Ref. 15,140–122, Gibco, Carlsbad, CA, USA), 1% Glutagro (Ref. 25–015-CI, Corning), and 10% of Fetal Bovine Serum (Ref. A5256701, Gibco).

Preparation of Serum-Free Medium

Serum-free media (SFM) for the proliferation (ProDuck4.0) or for the differentiation (LipoDuck2.0) of DEF were prepared by supplementing the basal medium with a proprietary non-disclosed formulation. The aforementioned media were developed using different Design of Experiments methodologies (DoE) to screen and optimize the components and were validated to sustain the proliferation and differentiation processes of DEF.

Serum-Free Media Composition

ProDuck4.0 and LipoDuck2.0 are serum-free proprietary media. They include insulin, transferrin, selenium, an albumin substitute, essential lipids/fatty acids, growth factors, and hormones. Exact compositions and supplier details are withheld under confidentiality. These general compositional characteristics are provided to aid the reproducibility of the study.

Adipogenesis Mix Preparation

Adipogenesis of the cells was induced by adding to the culture medium an adipogenesis mix (Lipomix) containing high concentrations of free fatty acids. For the preparation of the Lipomix, a magnetic stirrer was utilized to mix Tween 80 (Ref. P8074, MilliporeSigma), α-tocopherol acetate (Ref. 29,992, MilliporeSigma), and hydrolyzed linseed oil (Ref. 430,021, MilliporeSigma). Subsequently, water was gradually added to the mixture in a dropwise manner and after 10 min this mixture was added dropwise to 10% (*w/v*) Poloxamer 188 (Ref. 13–961-CI, Corning) with continuous magnetic stirring to allow the formation of the emulsion. Following the formation of the emulsion, it was subjected to filtration to ensure sterility using a PES syringe filter with a pore size of 0.22 µm. To preserve the stability and integrity of the Lipomix, it was stored at 4 °C and protected from light exposure.

Cell Culture Passaging and Maintenance

Regular subculturing was carried out using 25, 75, or 150 cm^2 culture-treated vented cap T-flasks. Cell cultures were maintained inside an ICO150 5% CO_2 humidified incubator at 37 °C (Memmert GmbH + Co. KG, Schwabach, Germany). Seeding density for cells growing in SSM was 7500 $cell{\cdot}cm^{-2}$ and for those growing in SFM was 15 000 $cells{\cdot}cm^{-2}$. Routinary observation and images were taken using a Motic AE31E LED Trinocular inverted microscope (Motic Optical, Xiamen, China). Media replacements were carried out every 2–3 days. The passaging procedure was performed upon reaching the desired confluency (> 90%), following the protocol outlined below.

Cells were gently washed three times with PBS −/−, avoiding excessive disruption of the cell monolayer. TrypLE Express 1X (Ref. 12,604,013, Gibco) was used as a dissociating agent and was incubated for 3–5 min at 37 °C. Detachment progress was monitored visually under an inverted microscope. To stop the reaction, twice the amount of TrypLE Express of room temperature (RT) proliferating cell culture medium was used. Finally, the cell suspension was centrifuged at 350 g for 6 min and resuspended in fresh culture medium to eliminate the detachment agent before subculturing.

Cell Culture on Microcarriers

Cytodex-1 microcarriers were used to grow the cells in unbaffled vented cap polycarbonate shake flasks (Ref. 431,143, Corning) or low attachment 6-well plates (Ref. 3471, Corning) to avoid cell attachment to the plastic surface, depending on the experiment. Cells were seeded maintaining a ratio of 11 cells/microcarrier (i.e. the concentration for 2 $g{\cdot}L^{-1}$ and 8600 $MC{\cdot}mL^{-1}$ of Cytodex-1 was of 100 000 $cell{\cdot}mL^{-1}$) in 12 mL in the shake flasks and in 2 mL in the 6-well plates. The shake flasks were placed in a Celltron 25 mm orbital shaker (Infors HT, Bottmingen, Switzerland) at 51 rpm inside a humidified 5% CO_2 incubator at 37 °C. Medium replacements (0.6 reactor volumes) were carried out every 2–3 days, following regular culture protocols in 2D. The media exchange was performed by letting the microcarriers settle in the bottom of the flask and then carefully eliminating the spent media using a serological pipette to then add the corresponding amount of fresh medium. When semi-perfusion protocols were applied, media replacements were carried out daily depending on cell concentration, following the protocol explained above.

Suspension Cell Concentration and Viability

Cell concentration and viability assays were carried out by the Nucleocounter-250 (NC-250, ChemoMetec, Allerod, Denmark), using the "Viability and Cell Count Assay" protocol according to the manufacturer's instructions.

Microcarrier-Adhered Cell Concentration and Viability

Concentration of cell adhered on microcarriers was determined using a modified version of the "Aggregated Cells Assay" from the NC-250. The protocol was modified by adjusting the counting gate to specifically include nuclei from DEF. A 100 µL homogeneous sample containing microcarriers was transferred to a 1.5 mL Eppendorf tube using a beveled pipette tip. The lysis of cells in the samples was carried out by the addition of Lysis Buffer A, and the nuclei were subsequently stabilized with Stabilizing Buffer B, following the manufacturer's instructions. The mixture of lysed cells was then counted to determine the total concentration of cells.

The cell concentration in the supernatant was determined by following the standard protocol for single-cell suspension. Finally, the concentration of microcarriers in the mixture was determined, allowing for further normalization by the concentration of microcarriers present in the cell culture. The total cells attached to the microcarriers (C_{att}), the % of cells attached ($\%_{att}$), and the cells·mL^{-1} normalized by the number of microcarriers (C·mL^{-1}) were calculated using the following equations:

$$C_{att} = \frac{C_t - C_{sn}}{MCs_s} \tag{1}$$

$$C/mL_c = C_{att} \times MCs_c \tag{2}$$

$$\%_{att} = \frac{C_{sn}}{C_t} \times 100 \tag{3}$$

where C_t is the total number of cells counted using the lysis protocol (cells·mL^{-1}), C_{sn} is the number of cells in the supernatant using the single cell counting protocol (cells·mL^{-1}), MCs_C is the theoretical concentration of microcarriers in the culture according to the manufacturer's manual (MCs·mL^{-1}), and MCs_s is the concentration of microcarriers in the counted sample (MCs·mL^{-1}).

Adipogenesis Induction Protocol in Shake Flasks and Stirred Tank Bioreactor

Adipogenic differentiation of cells growing on Cytodex 1 microcarriers in shake flasks (SF) was carried out by adding 2-HP-b-CD up to a final concentration of 3000 mg·L^{-1} in the proliferation medium. After that, a semi-perfusion protocol was carried out and a perfusion rate of 1.8 nL·cell^{-1}·day^{-1} was applied using LipoDuck2.0 supplemented with 1% Lipomix. This semi-perfusion was performed as described above, by daily allowing the microcarriers to settle at the bottom of the flask and carefully removing the corresponding spent medium using a serological pipette and replenishing with an equal volume of fresh medium to reach the CSPR of 1.8 nL·cell^{-1}·day^{-1}.

To differentiate the cells in the stirred tank bioreactor (STB), the feed bottle was used to add 2-HP-b-CD up to a final concentration of 3000 mg·L^{-1} in the proliferation medium. Then, the ProDuck4.0 medium was replaced by LipoDuck2.0 and slowly made a 0.6 RV medium replacement to avoid Lipomix-induced cell death. Once 0.6 RV of medium exchange was finished, a perfusion rate of 1.8 nL·cell^{-1}·day^{-1} was set.

Triglyceride Quantification

TG concentration was measured using a glycerol phosphate oxidase/peroxidase enzymatic test (Ref. 11,528, Biosystems, Barcelona, Spain) following the manufacturer's instructions. More information about the sample preparation and TG quantification protocol is in the Supplementary Material.

Fluorescence Microscopy

Aliquots from cultures were fixed with 4% paraformaldehyde (PFA) (Ref. 158,127, MilliporeSigma) in PBS for 15 min at RT followed by washing steps using PBS before storage at 4 °C until use. Nuclei were stained using 4′,6-diamidino-2 phenylindole dihydrochloride (DAPI) (Ref. D1306, Thermo Fisher Scientific) or 2′-[4′-etoxifenil]−5-[4-metilpiperazin-1-il]−2,5′-bis-1 h-benzimidazole trihydrochloride trihydrate (Hoechst) (Ref. 62,249, Thermo Fisher Scientific). In some cases, ActinRed 555 ReadyProbes reagent (Ref. R37112, Thermo Fisher Scientific) and 4,4-Difluoro-1,3,5,7,8-Pentamethyl-4-Bora-3a,4a-Diaza-s-Indacene (Bodipy) (Ref. D3922, Thermo Fisher Scientific) were used to stain the actin cytoskeleton and lipid droplets, respectively.

Images were taken using an Axiolab 5 fluorescence microscope (Zeiss, Carl Zeiss AG, Oberkochen, Germany) or a Leica TCS SP5 confocal microscope (Leica Microsystems GmbH, Wetzlar, Germany) depending on the experiment, and images were analyzed using IMARIS software (Version 9.5, Oxford Instruments, Abingdon, UK) and Fiji (Version 1.54f, National Institutes of Health, Bethesda, MD, USA).

Preparation of Materials and Microcarriers for 3D Cultures

Siliconization of glass surfaces (bottles and glass bioreactor tank) was performed to prevent microcarriers from adhering to glass surfaces. Briefly, glass vessels were cleaned to remove any contaminants by doing two sequential washes with 70% ethanol, followed by two washes with distilled water. The coating was carried out by repeatedly rolling the vessel for at least 10 min. The amount of

Sigmacote (Ref. SL2-100ML, MilliporeSigma) applied varied depending on the vessel size to ensure that the interior surface of each vessel was uniformly coated. Finally, the vessels were left to dry and then washed with distilled water to remove all remaining Sigmacote.

Cytodex 1 microcarriers (Ref. 17,044,802, Cytiva) 20 $g{\cdot}L^{-1}$ stock solution in PBS was prepared following the manufacturer's instructions and stored at 4 °C until use. Before their use in cell culture experiments, microcarriers were conditioned in culture media by exponential dilution. More information about microcarriers hydration, sterilization, and surface siliconization can be found in the Supplementary Material.

Rocking Motion Bioreactor

A BioStat B Rocking Motion bioreactor (RMB) (Sartorius Stedim Biotec, Göttingen, Germany) was used to cultivate DEF growing on Cytodex 1. The bioreactor was operated at 37 °C and the working volume was maintained at 0.75 L, with an air inlet flow rate set at 0.1 $L{\cdot}min^{-1}$. Oxygen saturation levels were not controlled (remained above 80% in all runs). When using Flexsafe RM 2L Basic single-use culture bags (Ref. DFB002L, Sartorius Stedim Biotech), the pH of the culture medium was manually regulated by adjusting the concentration of CO_2 in the gas inlet to meet a pH value of 7.2 measured using an off-line probe. When using Flexsafe RM 2L Optical or Flexsafe RM 2L perfusion single-use culture bags (Ref. DFO002L, DFP002L—SM, Sartorius Stedim Biotech), the 7.2 pH setpoint was controlled by the Digital Control Unit (DCU) using CO_2 and $NaHCO_3$ (7.5% *w/v*) with the bioreactor probe being recalibrated every 24 h utilizing an off-line probe.

The integrated filter within the culture bag was used as the cell retention device to carry out perfusion. The perfusion rate was adjusted daily, depending on the viable cell density, to meet a cell-specific perfusion rate (CSPR) of 1 $nL{\cdot}cell^{-1}{\cdot}day^{-1}$. Microcarrier concentration was 2 $g{\cdot}L^{-1}$. The control of the culture medium weight was carried out with a scale and pump integrated in the bioreactor DCU, which compensated for medium loss due to filtration processes by the addition of fresh media, thereby ensuring the maintenance of a constant working volume. The attachment protocol for the RMB was implemented as follows: an initial 30-min static incubation period, during which rocking was performed for 15 s every 10 min at a speed of 15 rpm and an angle of 10 degrees. This was followed by a 3-h static incubation period. After the attachment, two mixing conditions were performed at 4 degrees and 8 rpm and static conditions, with intermittent 15 s of mixing every 40 min at 10 degrees and 25 rpm.

Stirred Tank Bioreactor

A BioStat A STB (Sartorius Stedim Biotech) was used for DEF culture. The working volume within the bioreactor was maintained at 0.75 L, with a constant air inlet flow rate set at 0.1 $L{\cdot}min^{-1}$ and a constant temperature of 37 °C. pO_2 was controlled at 40% with oxygen pulses (remained above 80% in all runs with fixed overhead aeration only). The 7.2 pH setpoint was controlled by the DCU using CO_2 and $NaHCO_3$ (7.5% *w/v*). The bioreactor was equipped with a down-pumping 72° pitched 3-blade impeller (54 mm diameter) stirring at 50 rpm and an off-bottom clearance/tank diameter ratio (C/T) of 0.5 to ensure suspension of the microcarriers while reducing the shear stress (Loubière et al., 2019). The vessel had no baffles.

Perfusion was carried out by pumping out the medium directly from the dip tube, ensuring that the flow rate was low enough to avoid taking microcarriers out of the bioreactor. Microcarrier concentration was 2 $g{\cdot}L^{-1}$. Feed and harvest pumps were previously calibrated to ensure the same flow rate and therefore a constant working volume. The perfusion rate was adjusted on a daily basis depending on the viable cell density to meet a CSPR of 1 $nL{\cdot}cell^{-1}{\cdot}day\text{-}^{1}$.

Stoke's equations were used to calculate the critical flowrate (Q_c) that is governed by the settling rate of the particle. Assuming 25 °C, that the particles do not interfere with each other, and that the system is under laminar regime, the settling rate is calculated as follows:

$$v = \frac{2gr^2(\rho_p - \rho_f)}{9\eta} \tag{4}$$

where v is the settling velocity of the particle ($m{\cdot}s^{-1}$), g is the acceleration due to gravity (9.81 $m{\cdot}s^{-2}$), r is the radius of the spherical particles (1.6E-4 m), ρ_p is the density of the particle (1030 $kg{\cdot}m^{-3}$), ρ_f is the density of the fluid (density of water = 1000 $kg{\cdot}m^{-3}$), and η is the dynamic viscosity of the fluid (8.9E-4 $kg{\cdot}m^{-1}{\cdot}s^{-1}$):

Then, Q_c:

$$Q_c = A \times v \tag{5}$$

where A is the section of the tube (m^2) that has a radio of 0.005 m and v is the settling rate ($m{\cdot}s^{-1}$),

$$A = \pi r^2 \tag{6}$$

Therefore, taking into consideration these values and Eqs. 4, 5, and 6, the critical flowrate to avoid taking microcarrier particles out of the bioreactor was calculated to be 2.2 $mL{\cdot}min^{-1}$.

Orbitally Shaken Bioreactor

An SB10-X (Kühner Shaker AG, Birsfelden, Switzerland) orbitally shaken bioreactor (OSB) was used to culture DEF on Cytodex 1 microcarriers. The working volume within the bioreactor was maintained at 1.5 L, with a constant air inlet flow rate set at 0.2 $L{\cdot}min^{-1}$ and the temperature controlled at 37 °C. pO_2 was controlled at 40% with oxygen pulses. Microcarrier concentration was 2 $g{\cdot}L^{-1}$. The 7.2 pH setpoint was controlled by the DCU using CO_2 pulses and $NaHCO_3$ (7.5% *w/v*). A 3 L standard single-use bag with optical sensors (Ref. 105,332, Kühner Shaker AG) was used, and the orbital diameter of the shaker was set at 25 mm. The bioreactor probe was manually recalibrated every 24 h utilizing an off-line probe.

Perfusion was carried out by pumping out the medium directly from the harvesting tube ($r = 0.00463$ m), ensuring that the flow rate was low enough to not draw microcarriers out of the bioreactor ($Q \leq Q_c = 1.9$ $mL{\cdot}min^{-1}$), as in the STR. The feed and harvest pumps were calibrated to ensure the same flow rate and therefore a constant working volume. The attachment protocol for the RMB was implemented as follows: an initial 30-min static incubation period, during which shaking was performed for 60 s every 10 min at a speed of 80 rpm. This was followed by a 3-h static incubation period. After that, three different shaking speeds were tested in culture: 55 rpm, 80 rpm, and static conditions with 1 min of intermittent shaking at 80 rpm.

Determination of Glucose and Lactic Acid Concentration

Glucose and lactic acid concentrations in cell culture supernatants were measured using test strings (Ref. 116,720, 116,127, MilliporeSigma) and a Reflectometer RQ FLEX 20 (Ref. 117,246, MilliporeSigma) following manufacturer's instructions.

Data Analysis and Design of Experiments

Design of experiments (DoE) was carried out to optimize cell culture conditions. Central composite designs (CCD) were used to study the interactions between the significant factors and find optimal combinations. ANOVA analysis, fit statistics, and surface plots of the model were performed using Design-Expert 11 and can be found in Table S3 of Supplementary Material (Stat-Ease Inc., Minneapolis, MN, USA).

Cell-Specific Perfusion Rate Calculation

Cell-specific perfusion rate (CSPR), defined as the volume of medium exchanged per cell per day, was calculated as described in (Lavado-García et al., 2020). Briefly, it was calculated as

$$CSPR = \frac{F}{\left(C/mL_c \times V\right) \times t} \tag{7}$$

where F is the volume of medium exchange (mL), C/mL_C is the cell concentration attached to the MCs ($cells{\cdot}mL^{-1}$), V is the working volume (mL), and t is the time (days).

Results

Study of DEF Culture Conditions in Shake Flasks

First, we studied the ability of DEF to attach onto the surface of Cytodex 1 microcarriers when cultured in ProDuck4.0 medium. To that end, DEFs were detached from culture plates and seeded into 6-well low-attachment plates at a density of 100,000 $cells{\cdot}mL^{-1}$ with 2 mL at 2 $g{\cdot}L^{-1}$ of Cytodex 1 (11 $cells{\cdot}MCs^{-1}$ and 11,000 $cells{\cdot}cm^{-2}$) at a constant speed of 51 rpm. This speed corresponded to the minimum agitation required to keep microcarriers suspended in 125 mL shake flasks, as determined by visual observation. Attachment kinetics and efficiency were assessed by monitoring the cells in the supernatant, total cell count, and microscopy observations every 7 min.

At 7 min post-seeding, approximately 70% of the cells were associated with the microcarriers, with only 30% remaining in the supernatant (Fig. 2a). By 14 min post-seeding, almost all cells were attached to the microcarriers, and cell concentration in the supernatant stabilized, reaching a high attachment efficiency of 93.6% (Fig. 2a).

DEF growth kinetics on Cytodex 1 were studied in shake flasks to determine the optimal culture conditions. Cells were seeded into shake flasks at 51 rpm without medium replacements and under a semi-perfusion regime, and viability and cell growth were monitored over the culture period. Subsequently, cells were subjected to different agitation speeds, and cell growth rates were analyzed alongside microscopy observations of the microcarriers. After studying the seeding process, it was decided to implement a semi-perfusion approach, an operational strategy widely used in animal cell culture (Bielser et al., 2018; Gutiérrez-Granados et al., 2018). This strategy, consisting of medium replacement every 2–3 days, in line with routine 2D culture practices, was compared with batch culture conditions (Fig. 2b).

The analysis of cell growth revealed a 24-h lag phase after seeding, with a complete population doubling completed by 72 h post-inoculation (hpi), reaching 200,000 $cells{\cdot}mL^{-1}$ (Fig. 2b). In the condition with medium replacement, cells continued to grow, reaching 425,000

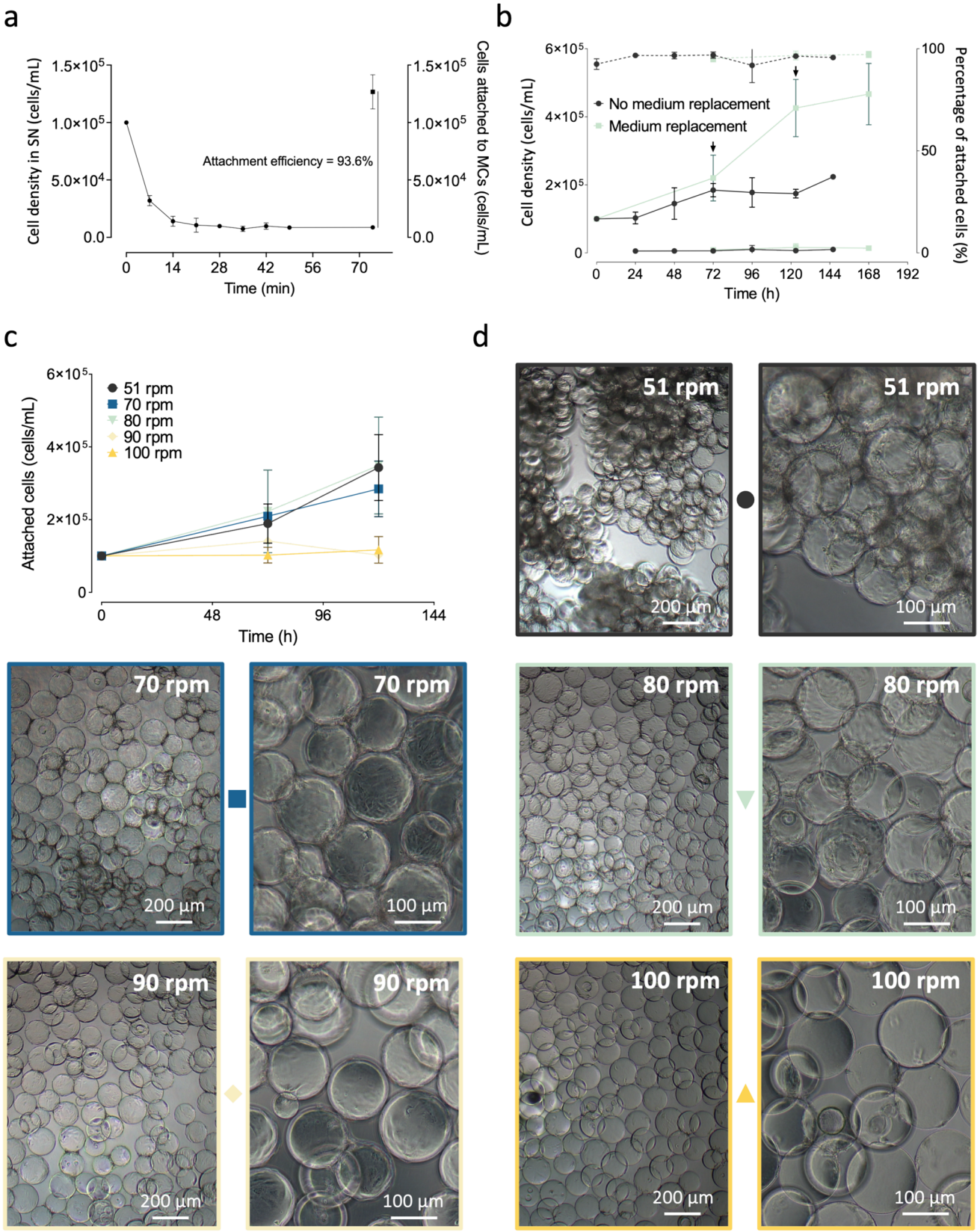
a
Cell density in SN (cells/mL)
1.5×10^5
1.0×10^5
5.0×10^4
0.0
Attachment efficiency = 93.6%
Cells attached to MCs (cells/mL)
0 14 28 42 56 70
Time (min)
b
Cell density (cells/mL)
6×10^5
4×10^5
2×10^5
0
No medium replacement
Medium replacement
Percentage of attached cells (%)
100
50
0
0 24 48 72 96 120 144 168 192
Time (h)
c
Attached cells (cells/mL)
6×10^5
4×10^5
2×10^5
0
51 rpm
70 rpm
80 rpm
90 rpm
100 rpm
0 48 96 144
Time (h)
d
51 rpm
200 µm
51 rpm
100 µm
70 rpm
200 µm
70 rpm
100 µm
80 rpm
200 µm
80 rpm
100 µm
90 rpm
200 µm
90 rpm
100 µm
100 rpm
200 µm
100 rpm
100 µm

◂**Fig. 2** Study of DEF culture conditions in shake flasks. **a** Cells in the supernatant (SN) (black dots) and total cell concentration (black squares) counted during the attachment process, performed using 2 g·L^{-1} Cytodex 1, low attachment 6-well plates at a continuous shaking speed of 51 rpm. **b** Attached and supernatant cell concentration (solid lines) and percentage of attached cells (viability) (dotted line) of DEF cultures growing in shake flasks at 51 rpm in ProDuck4.0 with medium exchanges every at 72 and 120 h (green squares) and in batch (black dots). Experiments performed three times in triplicate. **c** Cells attached to the microcarriers (MCs) at different shaking speeds: 51 rpm (black dots), 70 rpm (blue squares), 80 rpm (green inverted triangles), 90 rpm (yellow diamonds), and 100 rpm (yellow triangles). Experiments performed three times in triplicate except for 70 rpm ($n=1$) and 51 rpm ($n=8$). **d** Images of the cells at 120 h post-seeding at different shaking speeds

cells·mL^{-1} or 49 cells·MC^{-1} at 120 h, after which cell growth entered a stationary phase. In contrast, the condition without medium replacement remained around 200,000 cells·mL^{-1} or 23 cells·MC^{-1} for the rest of the culture period, indicating the need for media replacement to sustain cell growth beyond 72 hpi (Fig. 2b). The population doubling time (PDT) was 46 h, similar to that observed in 2D cultures, demonstrating the robustness of ProDuck4.0 in sustaining growth under different culture conditions. Cell viability remained above 90% in both conditions throughout the culture period (Fig. 2b).

Growth kinetics analysis at different agitation speeds showed significant differences in culture morphology and cell growth rate depending on the shaking speed. Cultures shaken at 90 and 100 rpm experienced complete inhibition of cell growth, indicating that these conditions exceeded the maximum shear stress tolerance of the cells. For shaking speeds of 51, 70, and 80 rpm, no major differences were observed (Fig. 2c).

Microscopy analysis of cell morphology and microcarrier aggregation revealed differences between culture conditions. Higher agitation speeds resulted in less aggregation, with cultures shaken at 90 and 100 rpm consisting almost entirely of clean microcarriers (Fig. 2d). At 80 rpm, cells covered the entire microcarrier surface, suggesting that the lack of aggregation observed at 90 and 100 rpm was related to agitation rate rather than cell growth or concentration. Conditions at 70 and 51 rpm showed more aggregation compared to the other conditions (Fig. 2d).

The attachment efficiency of DEF on Cytodex 1 was demonstrated to be high, with over 90% of cells attached. Proper proliferation of DEF was only achieved when culture media replacements were performed and when maintained within an agitation range of 51 to 80 rpm. Consequently, lower agitation (51 rpm) was adopted as the standard culture conditions for DEF.

Optimization of the Proliferation and Differentiation Processes in Shake Flasks

Prior to implementing the proliferation process at lab-scale bioreactor, the critical cell-specific perfusion rate ($CSPR_c$) was determined, considering that this is the most significant parameter influencing perfusion performance (Bielser et al., 2018). $CSPR_c$ is the minimum CSPR that maintains cell viability and supports proliferation without nutrient limitation or excess metabolite accumulation. When $CSPR < CSPR_c$, cell growth and viability decline due to insufficient medium exchange. When $CSPR \geq CSPR_c$, cultures can be sustained with stable metabolic conditions. To this end, DEF cultures growing on Cytodex 1 were seeded in shake flasks at a density of 200,000 cells·mL^{-1} and with 4 g·L^{-1} of Cytodex, maintaining the initial ratio of 11 cells·MC^{-1} and 11,000 cells·cm^{-2}. The initial seeding density and microcarrier concentration were increased in order to maximize the cell-to-media ratio and therefore the relative medium consumption, ultimately leading to a higher probability of finding the $CSPR_c$. Different medium replacement rates based on reactor volumes (RV) (ranging from 0.15 to 0.8 RV·day^{-1}) were applied. Cell growth and CSPR were monitored until the growth rate decreased, indicating the minimum threshold for maintaining optimal growth. At this point, the $CSPR_c$ was determined. CSPR was calculated as described in the "Materials and Methods" section.

Cell growth analysis indicated that the control condition, with no medium replacement, roughly completed a duplication at 48 hpi, after which cell concentration remained stable (Fig. 3a). Generally, all conditions exhibited similar behavior up to this time point, suggesting that medium replacements were not necessary for the first 48 h. However, 0.15 RV·day^{-1} was insufficient to sustain proper cell growth by 72 hpi, and 0.3 RV·day^{-1} became clearly limiting at 120 hpi. Only the 0.6 and 0.8 RV·day^{-1} conditions reached the maximum cell density of approximately $1{\cdot}10^6$ cells·mL^{-1}, with 0.8 RV·day^{-1} performing slightly better with up to $1.1{\cdot}10^6$ cells·mL^{-1} (Fig. 3a).

CSPR analysis evidenced that different conditions evolved towards a $CSPR_c$ of 0.779 nL·cell^{-1}·day^{-1}. The 0.15 RV·day^{-1} condition reached the limiting medium replacement at 48 h, 0.3 RV·day^{-1} at 96 h, and the 0.6 and 0.8 RV·day^{-1} conditions reached the limit between 120 and 144 h (Fig. 3b).

Once the $CSPR_c$ for proliferation was defined, a scalable protocol for differentiation in the microcarrier-based cell culture was developed and optimized. Based on previous work performed, where cells were differentiated in 2D cultures with periodic medium replacements using LipoDuck2.0 and Lipomix, a DoE response-surface methodology

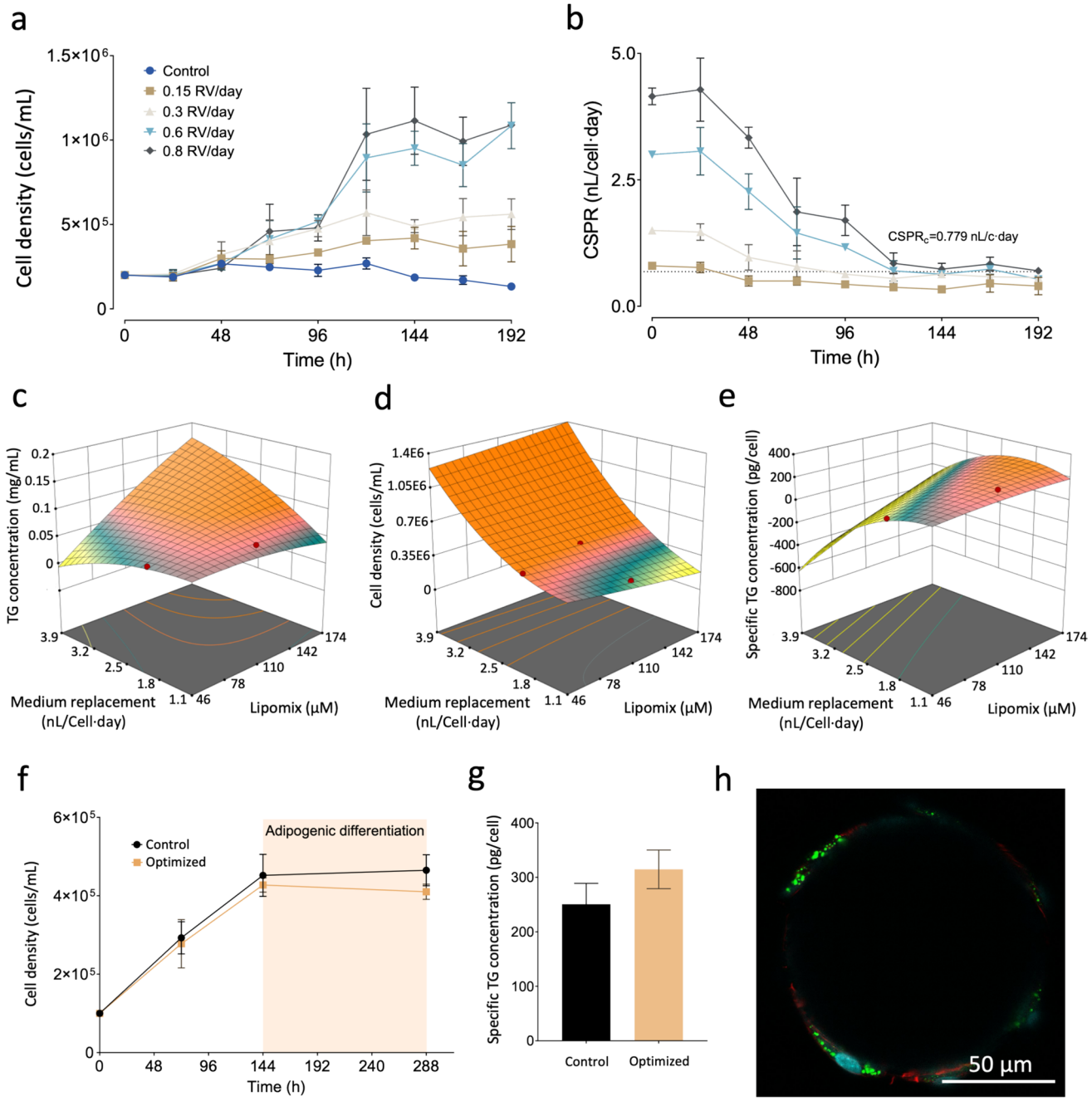

Fig. 3 Scale-up of the proliferation and differentiation processes in shake flasks. **a** Attached cell density of DEF cultured in ProDuck4.0 applying different medium replacement rates: 0.15 reactor volumes (RV)·day^{-1} (brown squares), 0.3 RV·day^{-1} (beige triangles), 0.6 RV·day^{-1} (cyan inverted triangles), 0.8 RV·day^{-1} (grey diamonds), and 0 RV·day^{-1} (C-) (blue dots). **b** CSPR through the culture period for the different medium replacements. The dotted line indicates a mean CSPRc of 0.779 nL·cell^{-1}·day^{-1}. Experiments performed twice in triplicate. **c–e** Response surface plots of the responses predicted by the model depend on the Lipomix concentration in the media and the CSPR. **f** Growth kinetics of the attached cells during the differentiation of the culture applying the non-optimized (black dots) and the optimized protocol (orange squares). Adipogenesis time indicated with an orange area. Experiments performed twice in triplicate. **g** Bar chart of the intracellular triglyceride accumulation at the end of the differentiation for the optimized condition. h. Confocal microscopy image of a single microcarrier 24 h after the beginning of the differentiation. Nuclei are shown in blue; b-actin is shown in red and lipid droplets are shown in green

(Supplementary Material Table S3) was employed to assess the effects of Lipomix concentration and CSPR on cell survival and specific triglyceride (TG) accumulation. 6-well plates with a working volume of 2 mL·well^{-1}, 2 g·L^{-1} of Cytodex 1 and a seeding density of 100,000 cells·mL^{-1} was used. Following the optimization, the new operational strategy was validated through TG measurement and confocal microscopy analysis.

The analysis of TG concentration at the end of the culture revealed a significant positive effect of Lipomix concentration, whereas medium replacement did not significantly influence TG concentration (Fig. 3c). There was a clear positive interaction between Lipomix concentration and medium replacement (Fig. 3c). In terms of cell survival, only medium replacement had a positive influence, with no significant interaction between the two factors (Fig. 3d). For specific TG accumulation, both Lipomix concentration and the two-factor interaction positively impacted the response (Fig. 3e).

The obtained model for specific TG accumulation was used to refine the differentiation strategy, balancing high cell survival with overall TG concentration. This yielded an optimal condition of 167 µM of Lipomix in the culture medium and an optimal CSPR of 1.83 nL·cell^{-1}·day^{-1}. The optimized conditions resulted in a final specific TG accumulation of 314 pg·cell^{-1}.

Confocal microscopy images obtained from single microcarriers in 24 h post-differentiation (hpd) cultures demonstrated the ability of the cells to accumulate lipid droplets from the early stages of the differentiation process, as can be seen in green in the image (Fig. 3h). During the initial development of the differentiation protocol in 2D cultures, the process was validated by analyzing the expression of key adipogenic markers (PPARg, C/EBPa, and FABP4) using qPCR, observing a clear upregulation of PPARg and FABP4 (Supplementary Fig. S1). This molecular validation step confirmed the robustness of the differentiation protocol, although for subsequent optimization and high-throughput screening studies only TG accumulation and BODIPY staining were used.

Therefore, a new proliferation protocol with a constant perfusion rate of 1 nL·cell^{-1}·day^{-1} to ensure sufficient medium replacement was established, together with an optimal strategy for the differentiation of DEF in shake flasks, consisting of a CSPR of 1.83 nL·cell^{-1}·day^{-1} and a Lipomix concentration of 167 µM.

DEF Culture at Bioreactor Scale

To study the proliferation in the RMB, various combinations of rocking speed and angle were tested, leading to different levels of microcarrier mixing. Following the characterization by Thomassen et al. (2012), who described nine levels of homogeneity in a Biostat Cultibag RMB, conditions equivalent to levels 7–9 (indicating homogeneous suspension of microcarriers) were selected. This strategy ensured sufficient mixing while limiting agitation, in line with the just-suspended criterion applied throughout this study for bioreactor scale-up.

No cell growth was observed when cultivating the cells under continuous rocking, after the attachment phase, at 8 rpm and 4°, with complete cell death observed by 48 hpi (Supplementary Fig. 2a, b). Consequently, a static condition (periodic homogenization of 15 s at 25 rpm, 10° every 40 min) was tested. In this case, the culture survived 24 h longer than in the continuous rocking condition, but the cells died after 72 h of culture (Supplementary Fig. 2c, d).

In both experiments, the initial cell density was lower than the usual 100,000 cells·mL^{-1} used in other experiments (Supplementary Fig. 2a, c). The lack of growth under conditions that were successful with SSM led to considering that the seeding density might be too low. Therefore, an experiment under semi-static conditions was conducted, doubling the seeding density to 200,000 cells·mL^{-1} while maintaining the microcarrier concentration. By doing this, although the cells experienced a sharp decrease in viability during the first 48 h, the culture recovered over the next 48 h, reaching the initial cell concentration and entering a plateau that lasted for 96 h until the experiment was stopped (Supplementary Fig. 2e, f). These findings indicate that DEF show a high sensitivity to agitation in the RMB, even at low rocking speeds.

Experiments similar to those performed in the RMB were carried out: one static condition with periodic shaking to homogenize the culture, one with the minimum shaking speed to keep the microcarriers (and cells) fully suspended, and another with low shaking and poor microcarrier mixing. In all runs, perfusion was started after 24 h through one of the dip-in tubes of the bioreactor single-use bag, as explained in the "Materials and Methods" section. Pump flow rate was adjusted daily to apply the previously determined CSPR and the waste bottle was monitored to ensure no microcarriers were being lost from the bioreactor. The mixing threshold was determined by visual assessment of microcarrier sedimentation, with 80 rpm identified as the minimum speed for homogeneous suspension, a criterion also used in other microcarrier studies (Lawson et al., 2017; Rafiq et al., 2013; Thomassen et al., 2012).

The condition with good microcarrier mixing yielded results similar to those observed in the RMB: the cells did not survive beyond 72 h post-seeding (Supplementary Fig. 3a, b). Lowering the shaking speed to reduce shear stress, even at the cost of microcarrier homogeneity, was further tested. Experiments cultivating the cells at 55 rpm with continuous shaking were carried out, showing no significant improvement, with nearly all cells dead at 48 hpi (Supplementary Fig. 3c, d).

a

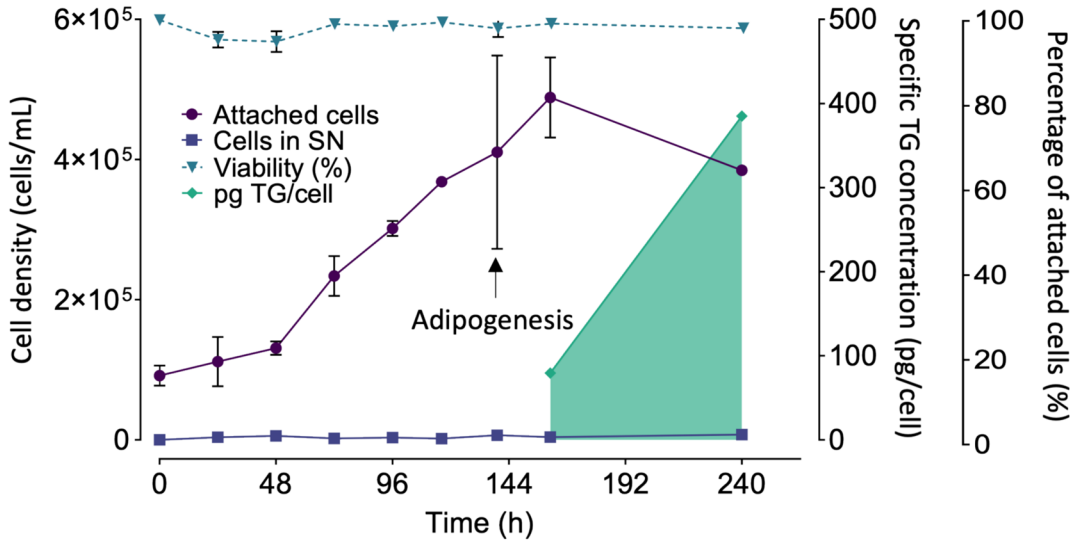
Cell density (cells/mL)
6×10^5
4×10^5
2×10^5
0
Attached cells
Cells in SN
Viability (%)
pg TG/cell
Adipogenesis
0
48
96
144
192
240
Time (h)
500
400
300
200
100
0
Specific TG concentration (pg/cell)
100
80
60
40
20
0
Percentage of attached cells (%)

b

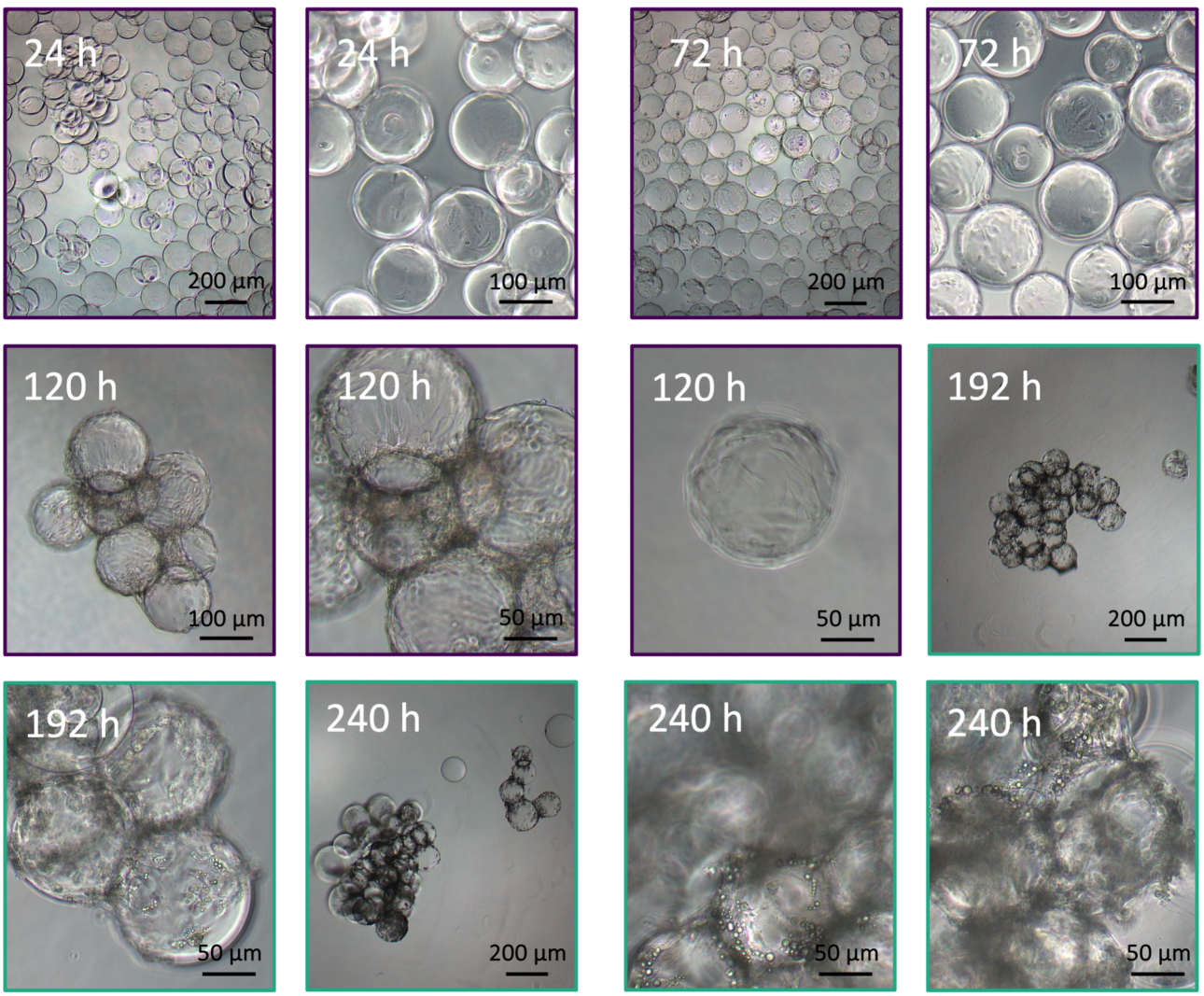
24 h
200 µm
24 h
100 µm
72 h
200 µm
72 h
100 µm
120 h
100 µm
120 h
50 µm
120 h
50 µm
192 h
200 µm
192 h
50 µm
240 h
200 µm
240 h
50 µm
240 h
50 µm

◂**Fig. 4** Scale-up of DEF proliferation and differentiation in a stirred tank bioreactor. **a** Growth kinetics of DEF growing on Cytodex-1 microcarriers in a 1 L STB (0.75 L working volume) operating in perfusion mode (1 and 1.83 nL·cell^{-1}·day^{-1} for proliferation and differentiation, respectively). Microcarrier concentration was 2 g·L^{-1} in all the experiments. Proliferation experiment carried out three times and differentiation experiment one time. Dotted line indicates viability (blue inverted triangles), green area indicates intracellular triglyceride accumulation (green diamonds), and solid lines indicate cells attached to the microcarriers (burgundy dots) and cells in the supernatant (purple squares). **b** Images of the cells cultured in the bioreactor at different time points during the proliferation (burgundy frames) and the differentiation (green frames) phases

These results led to testing less ideal culture conditions: static culture with homogenization every hour at 80 rpm. This approach showed a clear improvement over the other conditions, with sustained cell viability for a longer period. However, despite prolonged cell survival, no cell growth was observed for 144 h (Supplementary Fig. 3e, f).

These findings suggest that the OSB, despite its similarity in shaking conditions with the shake flasks, is not an optimal bioreactor typology for the culture of DEF, suggesting that DEF are very sensitive to agitation even at laboratory scales.

Finally, the STB was evaluated to determine if this agitation technology could support cell growth. The impeller configuration was modified following the model described by Loubière et al., 2019 adjusted to the bioreactor used in this study. This configuration was empirically validated through visual observation of the microcarriers mixing in the STB. The microcarrier concentration was 2 g·L^{-1} and the impeller speed was set to 50 rpm, corresponding to the minimum condition that ensured full suspension of the microcarriers while limiting stress. The bioreactor operated in perfusion mode through the dip-in tube ensuring that no microcarriers were lost during the process, as in previous experiments. Attached cells, cells in the supernatant, viability, and cell morphology through the experiment were studied.

This bioreactor type was able to sustain the proper proliferation of DEF, allowing them to reach full confluence on the microcarriers. The attached cells experienced a relatively long lag phase at the beginning of the culture, followed by a growth phase with a doubling time of 58 h, slightly higher than in shake flasks. Cell density peaked at 168 hpi at 489,000 cells·mL^{-1}, concomitant with previous results (Fig. 2b). Viability analysis showed that the percentage of attached cells remained near 100% throughout the culture period, with very few cells in the supernatant (Fig. 4a).

Visual analysis of the culture revealed significant changes in cell morphology and aggregation over time. Images taken at 24 hpi showed cells with proper morphology homogeneously attached to the microcarriers (Fig. 4b). At 72 hpi, most microcarriers were showing at least 40% confluence, and aggregation had not yet begun. This changed at 120 hpi, where cells began to form aggregates after reaching full confluency on the microcarriers (Fig. 4b).

Successful cell proliferation in the STB led to the assessment of DEF differentiation in this bioreactor type. Adipogenesis was started at 144 hpi and about 400 000 cells·mL^{-1}, 24 h before the cells reached their peak density following the protocol developed earlier, and specific TG accumulation was assessed, in addition to the other parameters monitored during the proliferation phase.

Just 48 h post-differentiation (hpd), cells started accumulating lipid droplets, which significantly increased in size and quantity by the end of the culture at 96 hpd (Fig. 4b). After the peak of cell density, the concentration started to slowly decrease until it reached the concentration of the beginning of differentiation, while specific TG accumulation rose to 380 pg·cell^{-1}, reaching values similar to those observed in shake flasks (Fig. 2g).

These results demonstrate that the STB operating in perfusion mode can sustain the growth and adipogenesis of DEF using the serum-free media ProDuck4.0 and LipoDuck2.0. Cell densities comparable to those achieved in shake flasks were attained, along with similar TG accumulation.

Discussion

Shake Flask Cultures Reveal Shear Sensitivity of DEF on Cytodex 1 Microcarriers

Experiments analyzing the attachment efficiency and growth kinetics on Cytodex 1 microcarriers using the in-house proprietary serum-free media demonstrated the ability of DEF to proliferate in shake flasks. While the culture of chicken embryonic fibroblasts (CEF) on Cytodex 1 has been documented (Hundt et al., 2005; Zhang et al., 1997), this study is the first to address DEF culture on microcarriers. DEF isolated from Khaki Campbell ducks could efficiently attach, spread, and proliferate on Cytodex 1 microcarriers in a serum-free environment.

DEF failed to proliferate at shaking speeds higher than 80 rpm, indicating sensitivity to shear stress conditions, a phenomenon well-documented in the literature for cells cultured on microcarriers (Grein et al., 2019). Some works on microcarrier cell cultures have observed that the minimal shaking speed for the complete suspension of Cytodex 1 is 70 rpm in 125 mL shake flasks (25 mL working volume), slightly higher than the 51-rpm minimum shaking speed (10–12 mL working volume) empirically determined in this work (Maillot et al., 2022).

Shear stress arises from microturbulence in the culture media, caused by agitation. In the fluid, eddies of different sizes are formed and those having the size of cells can

directly interact with cell membranes, causing senescence, apoptosis, and necrosis (Cherry & Papoutsakis, 1986; Croughan et al., 1989; Koh et al., 2020). Larger eddies, however, can encompass entire microcarriers, reducing shear forces on the cell surfaces (Cherry & Papoutsakis, 1986; Croughan et al., 1986). The sensitivity to shear stress is more pronounced in microcarrier cultures compared to single-cell suspensions due to the higher freedom of movement in the former, which allows the cells to freely move with the eddies.

Shear stress is not only a physical concern, causing cell membrane rupture and death, but also a physiological signal sensed by cells via specific receptors, leading to significant changes in cellular function (Kunnen et al., 2018). This phenomenon has been extensively studied in both biomanufacturing and physiological contexts, such as in endothelial cells within blood vessels (Chu & Peters, 2008). Interestingly, low to moderate shear stress levels can enhance recombinant protein production in HEK293 cells cultured in bioreactors operating in perfusion using a hollow fiber cassette (Zhan et al., 2020). The improvement of physiological conditions under low shear stress have been reported in different studies using diverse cell types, including human fibroblasts (Wang & Thampatty, 2006). However, it is widely accepted that high shear stress levels generally have negative effects on cell physiology (Grein et al., 2019; Julaey et al., 2016; Zhan et al., 2020). The possible benefits of low shear stress have not been addressed here, where only the maximum shear stress was determined to be at around 90 rpm in shake flasks. Hence, future work with a more in-depth characterization of the cellular response to the range of agitation studied here should be carried out to gain knowledge of this phenomenon, similar to the work carried out in other studies (Chu & Peters, 2008; Kunnen et al., 2018; Qiao et al., 2016; Yamamoto et al., 2020; Zhan et al., 2020).

Design space in terms of shaking speed for the culture of microcarriers of DEF has been established. This small-scale system was useful for studying the proliferation and differentiation of DEF as a previous step for the implementation of the culture in the bioreactor and helped to gain insights into cell sensitivity to shear stress conditions.

Development of a Successful Proliferation and Differentiation Process Using Serum-Free media

Combining CSPR analysis and DoE-based assessments of both CSPR and Lipomix concentration in the culture, the proliferation and differentiation protocols in shake flasks could be developed and validated. $CSPR_c$ is a crucial parameter in driving perfusion processes (Bielser et al., 2018). Various studies have established methodologies for determining $CSPR_c$, particularly for suspension immortalized cell lines like CHO or HEK293 cells (Lavado-García et al., 2020; Maria et al., 2023). Typically, CHO cells exhibit a CSPR ranging from 15–70 $pL{\cdot}cell^{-1}{\cdot}day^{-1}$ in commercial media (Bielser et al., 2018). In contrast, DEF cells displayed a CSPR of 793 $pL{\cdot}cell^{-1}{\cdot}day^{-1}$ during the growth phase and 1830 $pL{\cdot}cell^{-1}{\cdot}day^{-1}$ during differentiation, significantly deviating from the literature. The proliferation and differentiation protocols optimized in this work set the foundation for further optimization of the production system, as a first step for a future scale-up of the production.

Scale-Up of the Process to Bioreactor Showed Disparities Across the Agitation Systems Tested

The assessment of the RMB to sustain the growth of DEF yielded no cell growth at all when the cells were cultured in continuous rocking and using ProDuck4.0. RMBs are known for their lower shear stress and comparable oxygen transfer and power inputs relative to traditional systems, making them widely used in both laboratory and industrial settings for animal cell cultures (Wierzchowski & Pilarek, 2024).

Given the specificity of the studied system, where a duck primary cell line is cultivated on Cytodex 1 microcarrier and in a proprietary serum-free medium, finding comparable results is challenging from a biological perspective. Most studies using microcarriers in RMBs focus on mesenchymal stromal cells (MSCs). Some of them reported reduced shear stress compared to stirred bioreactors and despite suffering from mixing and aggregation challenges (de Sá Silva et al., 2019; Tsai et al., 2017), achieved MSCs expansion while maintaining good viability and differentiation potential (Koh et al., 2020; Panchalingam et al., 2015). Another work on MSCs expansion described the successful growth of MSC with expansion factors (EF) ranging from 11.7 and 25.6 with agitation rates of 24 rpm and 4° (de Sá Silva et al., 2019).

Research by Timmins et al., 2009, 2011, 2012) found that cultures of umbilical cord blood hematopoietic stem cells and human placental MSCs faced proliferation issues when inoculated at low cell densities in an RMB due to over-oxygenation of the culture medium and shaking. This issue was mitigated by increasing the seeding density and limiting the dissolved oxygen (DO) to 50% for the hematopoietic stem cells (Timmins et al., 2009). Nonetheless, in MSCs cultures, where a static pre-amplification phase in shake flasks was added to increase the seeding density, the performance was still very poor. The problem was only overcome when the DO % was limited to 50% (Timmins et al., 2012). Increasing the seeding density did not result in cell growth in the conditions tested in this work. However, the effect of reducing the DO on culture performance was not explored and remains to be addressed in the future. However, similar DO levels, near 100% saturation, were observed across all bioreactor systems, indicating that elevated oxygen concentration alone

is unlikely to account for the reduced performance observed in the RMB.

Other cell lines have been successfully cultured using RMB systems. Immortal CP5 bovine chondrocyte cultures have been scaled up to RMB by using the Reynolds number and oxygen mass transfer coefficient (kLa) as predictors of cell performance (Wierzchowski et al., 2021). Literature on Vero and MDCK cells cultured in this bioreactor typology using Cytodex 1 is also available within the scope of vaccine production. In this case, the scalability of the system to a 20 L RMB was demonstrated with EF as high as 5 obtained and a PDT of 41 h (Genzel et al., 2010; Schouwenberg et al., 2010; Thomassen et al., 2012). A comparative study for the scale-up of Vero and HEK293 cultures using Cytodex-1 in a Wave25 bioreactor showed good results for the expansion of Vero cells, while HEK293 could not proliferate in any of the culture conditions tested, indicating high dependency on the used cell line (Yang et al., 2019). Based on the experiments presented here, and in contrast to the successful expansion of other cell lines in RMB, it appears that the main limitation lies in the DEF cells themselves.

The OSB also failed to sustain cell growth on microcarriers, producing results similar to those observed with the RMB. Previous studies have investigated the mixing conditions and critical shaking speeds necessary to maintain good mixing while reducing shear forces in microcarriers within orbitally shaken systems (Olmos et al., 2015; Pieralisi et al., 2016). These studies have extensively described the hydrodynamic phenomena affecting microcarriers in fluids but have not focused on the cultivation of cells. Other studies have successfully cultured cells in orbitally shaken systems, but these were primarily conducted using shake flasks or other small-scale systems, where we did not encounter significant cultivation issues either (Földes et al., 2021; Goh et al., 2013; Jeske et al., 2021; Maillot et al., 2022; Rodrigues et al., 2013; Sion et al., 2020). Some of these works have cultured MSCs at similar shaking speeds to those used in this research, probably indicating a limitation in maximum shaking speed to obtain proper cell growth and viabilities (Maillot et al., 2022). To our knowledge, this is the first work describing the use of laboratory-scale bioreactors, like the 3 L bag with a 1.5 L working volume used in this study, for anchorage-dependent cells on microcarriers. Therefore, contextualizing the results obtained here is challenging, as it is difficult to determine whether they are typical or exceptional. However, considering the results obtained with the RMB, it appears that our system is particularly sensitive to scale-up conditions.

The STB was the only bioreactor typology that achieved cell proliferation and differentiation, yielding results similar to those obtained in shake flasks. STBs are the gold standard in biomanufacturing, widely used at large scales (Xing et al., 2009). Several studies have established protocols for the culture of anchorage-dependent cells such as Vero and HEK293 in stirred tank bioreactors using microcarriers from laboratory to 200 L scales (Genzel et al., 2010; Yang et al., 2019). However, as discussed earlier, different cell lines and culture media may yield different results when cultivated in the same bioreactor.

Other studies have addressed the cultivation of MSCs and CEF, cell lines similar to DEF, in STBs. These studies proposed new impeller configurations to mitigate shear stress in the case of MSCs, achieving cell concentrations comparable to or lower than those obtained in this work (Hewitt et al., 2011; López-Fernández et al., 2024; Loubière et al., 2019; Zhang et al., 1997). Although successful in cultivating these cell lines, it is important to note that adjustments to the bioreactor design were necessary to achieve these results, indicating a high sensitivity to shear stress conditions that has been widely described in the literature for adherent cell cultures (Cherry & Papoutsakis, 1986; Collignon et al., 2016; Croughan et al., 1986, 1989; Julaey et al., 2016; Papoutsakis, 1991; Sion et al., 2020). Another study on MSCs demonstrated the scalability of the culture system up to a 5 L bioreactor (2.5 L working volume) (Rafiq et al., 2013). More recently, research by Lawson et al., 2017 described fed-batch expansion of primary human MSCs in a 50 L single-use stirred tank bioreactor using microcarriers, reaching harvest densities of $2.56 \cdot 10^5$ cells·mL^{-1} and total cell yields of $1.28 \cdot 10^{10}$. The authors emphasized that scale-up was only possible through careful management of hydrodynamic parameters, using P/V and impeller tip speed as criteria, highlighting the sensitivity of primary adherent cultures to shear stress in dynamic conditions. Still, most research focuses on small-scale stirred systems such as miniaturized bioreactors and spinner flasks, which are suitable for autologous cell therapies, with limited availability of published data on pilot or industrial scales culture of primary cells and no literature addressing the culture at large scale of any anchorage-dependent cell. In this context, it is worth noting that spinner flasks, often used as predictive scale-down models for STB processes, were not available for this study. Their inclusion could have provided a more representative model of the cultivation in STB, although the consistency observed between shake flask and stirred systems indicates that the chosen approach was still informative for process development.

To contextualize these findings, a comparison of microcarrier-based bioreactor systems reported in the literature comparable to the ones used in this work is compiled in Table 1. This summary highlights operation mode, performance metrics, and key hydrodynamic parameters, enabling direct comparison between RMB, OSB, and STB systems across different adherent cell types.

Table 1 Comparison of microcarrier-based systems for adherent cell culture: operation modes, scales, and hydrodynamic parameters reported in the literature and in this study

System	Operation mode	Cell type	Microcarrier	Performance metric	Working volume	Hydrodynamics	Reference
STB (XDR-50)	Semi-perfusion (partial medium replacement)	HEK293T	Cytodex-1	1.5×10^6 cells·mL^{-1} (peak, d4)	32 L	40 rpm; P/V 6 W·m^{-3}; DO 40%; pH 7.1	(Yang et al., 2019)
STB (XDR-200)	Semi-perfusion (partial medium replacement)	Vero	Cytodex-1 (g)	3.3×10^6 cells·mL^{-1} (peak, d4.5)	106 L	60 rpm; P/V 6 W·m^{-3}; eddy size 90–95 µm; DO 40% ± 10%; pH 7.0 ± 0.2	(Yang et al., 2019)
STB (5 L vessel)	Semi-perfusion (partial medium replacement)	hMSC (BM, primary)	Plastic P-102L	1.7×10^5 cells·mL^{-1} (6–sevenfold, peak d10)	2.5 L	3-blade 45°-pitch wide blade impeller (D = 70 mm) and four vertical baffles. DO > 45%; pH 7.2 → 6.7; 75 rpm	(Rafiq et al., 2013)
STB (1 L benchtop)	Semi-perfusion (partial medium replacement)	hfMSC (fetal, primary)	Cytodex-3	$6–8\times10^5$ cells·mL^{-1} (12–16-fold, peak, d8),	0.5 L (d0-1), 1 L (d1-8)	30 rpm (d0-1), 50 rpm (d1-8), DO 30%, pH 7.2–7.3	(Goh et al., 2013)
STB (spinner flask)	Semi-perfusion (partial medium replacement)	HEK293T/Vero	Cytodex-1	3.5×10^6 cells·mL^{-1} (peak, d3-5)/2×10^6 cells·mL^{-1} (peak, d3-5)	1000 mL	55 rpm	(Yang et al., 2019)
STB (2 L single-use benchtop)	NS*	hMSC (BM, primary)	NS*	5.3×10^5 cells·mL^{-1}, (peak, d9)	2 L	70 rpm; DO < 20%, pH 7.2. P/V 1.24 W·m^{-3} Increased impeller blade, lowered off-bottom clearance	(Jossen et al., 2014)
STB (50 L single-use pilot)	Fed-batch	hMSC (BM, primary)	Collagen-coated (PALL)	1.9×10^6 cells·mL^{-1} (peak, d11)	50 L	67 rpm; P/V 2–5 W·m^{-3}; DO 80%; pH 7.45, Max. Eddy 114	(Lawson et al., 2017)
RMB (WAVE 25)	Semi-perfusion (partial medium replacement)	Vero	Cytodex-1 (g)	2.8×10^6 cells·mL^{-1} (peak, d4)	8 L	12 rpm, 6° (d0–2), 15 rpm afterwards	(Yang et al., 2019)
RMB (WAVE 25)	Semi-perfusion (partial medium replacement)	HEK293T	Cytodex-1	Failed attachment. No cell growth	8 L	12 rpm, 6° (d0–2), 15 rpm afterwards	(Yang et al., 2019)
RMB (1 L)	Fed-batch, semi-perfusion	hMSC (BM, primary)	CultiSpher-S	Maintained up to d100 (peak at d40)	200 mL	15 rpm (d0-1), 30 rpm (d > 1–100)	(Nguyen et al., 2019)
RMB (1 L)	Batch	CP5 chondrocytes	Cytodex-3	$31.21\cdot10^8$ cells·m^{-2}, 1 mg/mL MC (equivalent to about $1.37\cdot10^6$ cells/mL)	300 mL	20 rpm; 6°; DO remained 100% in the culture (no control), pH 7.1	(Bartczak et al., 2022; Wierzchowski et al., 2021)

Table 1 (continued)

System	Operation mode	Cell type	Microcarrier	Performance metric	Working volume	Hydrodynamics	Reference
OSB (125 mL shake flask)	Fed-batch	DPSC (primary)	Cytodex-1/Cytopore-2	3×10^7 cells per flask, sixfold, (peak, d7)	43 mL (d0-2), 68 mL (d2-7)	100 rpm	(Földes et al., 2021)
OSB (125 mL shake flask)	Semi-perfusion (partial medium replacement)	WJ-MSC (primary)	Cytodex-1	$2{\cdot}10^6$ cells/flask (peak, d13)	25 mL	70 rpm	(Sion et al., 2020)
This manuscript (1 L STB)	**Perfusion**	**DEF (primary)**	**Cytodex-1**	**0.489×10^6 cells·mL^{-1} (2 g/L MCs)**	**0.75 L**	**50 rpm; DO remained > 90% in the culture (no control); pH 7.2, CSPR_prolif = 1.0 nL·cell^{-1}·day^{-1}; CSPR_diff = 1.83 nL·cell^{-1}·day^{-1}**	**This manuscript**
This manuscript (1 L RMB)	**Perfusion**	**DEF (primary)**	**Cytodex-1**	**Growth limited; strong shear sensitivity**	**0.75 L**	**20 rpm; 6° rocking; perfusion with retention DO remained > 90% in the culture (no control); pH 7.2; CSPR_prolif = 1.0 nL·cell^{-1}·day^{-1}**	**This manuscript**
This manuscript (4 L OSB)	**Perfusion**	**DEF (primary)**	**Cytodex-1**	**Growth limited; no sustained proliferation vs STB**	**1.5 L**	**90 rpm orbital; perfusion with retention; uneven suspension DO remained > 90% in the culture (no control); pH 7.2; CSPR_prolif = 1.0 nL·cell^{-1}·day^{-1}**	**This manuscript**
This manuscript (125 mL shake flask)	**Semi-perfusion**	**DEF (primary)**	**Cytodex-1**	**1.1×10^6 cells·mL^{-1} (4 g/L MCs)**	**10–12 mL**	**51 rpm (10–12 mL); no growth > 80 rpm**	**This manuscript**

**NS* not specified

The limited performance of wave-mixed and orbitally shaken systems is consistent with previous reviews on shear-sensitive stem and stem-like cells, a category that includes embryonic fibroblasts. These studies highlight that, while wave and orbital systems provide gentle mixing, their scalability and compatibility with microcarriers are limited (Nogueira et al., 2021; Olmos et al., 2015). In contrast, stirred tanks are considered the most robust platform for adherent cell expansion when operated close to the just-suspended speed to balance suspension and shear, especially because they offer more flexibility regarding shear and mass transfer control (Jossen et al., 2016; Loubière et al., 2019; Teale et al., 2023). Therefore, the results reported here confirm established observations that STBs offer the best compromise for shear-sensitive cells in dynamic culture.

Despite the positive results achieved with the STB operating in perfusion, it presents several limitations that should be addressed in the future to achieve the scalability of the production process. Key challenges include shear stress sensitivity, surface growth limitation on the microcarriers leading to low cellular yields, and the lack of available research on the culture of DEF. Also, the perfusion methodology described here in the cases of the STB and OSB has limited scalability when increasing bioreactor size or microcarrier concentration. Nonetheless, it has proven very useful for preliminary studies and early process development as the one carried out in this work since it requires almost no optimization.

Limitations, Prospects, and Challenges

A major challenge in comparing different culture platforms lies in the accurate quantification of shear stress and other hydrodynamic parameters, which varies with vessel geometry, agitation method, working volume, fluid properties, and impeller configuration. While empirical determination of agitation limits provided practical guidance in this study, future work should incorporate direct hydrodynamic measurements, such as computational fluid dynamics, particle image velocimetry, or torque-based analyses, to better define shear profiles. Integrating these measurements with in-depth cell biology studies (i.e., transcriptomics or proteomics studies) will help clarify how mechanical forces influence cell phenotype under these dynamic conditions.

An additional limitation of the present study is the use of Cytodex 1, which is not edible and therefore not directly applicable for human consumption. In parallel to this study, our research group developed edible microcarriers composed of alginate matrices functionalized with polysaccharides. Cytodex 1 was used here to establish and optimize culture conditions in a reproducible platform, with the strategy of subsequently adapting these processes to the edible microcarriers. We have already confirmed that DEF can attach, proliferate, and undergo adipogenic differentiation on the edible microcarriers under static and semi-static culture conditions in the RMB (unpublished results). The next step will be to evaluate performance under dynamic conditions and confirm food safety compliance.

The growth of DEF on the surface of microcarriers as a strategy to scale up the proliferation and differentiation processes has been demonstrated. Perfusion was demonstrated to be a feasible strategy in shake flasks. By combining a semi-perfusion methodology with DoE, the optimal CSPR for both proliferation, 1 $nL \cdot cell^{-1} \cdot day^{-1}$, and differentiation, 1.83 $nL \cdot cell^{-1} \cdot day^{-1}$, using serum-free media could be determined.

Various bioreactor typologies were tested to scale up the culture from shake flasks to lab-scale bioreactors. Growth using RMB and OSB could not be achieved despite the several tests performed. However, DEF proliferation and differentiation were achieved in a STB, reaching cell densities and intracellular TG accumulations comparable to those obtained in shake flasks.

Overall, this study demonstrates the feasibility of cultivating duck primary cells on microcarriers in a stirred tank bioreactor under serum-free conditions. These findings establish a first proof of concept for duck fat production in bioreactors and provide a foundation for future work toward process intensification and scale-up.

Supplementary Information The online version contains supplementary material available at https://doi.org/10.1007/s11947-026-04259-4.

Author Contribution ADM conceived the study, designed the methodology, performed data analysis, and wrote the manuscript. AC, JF, NI, NG, and YE contributed to data collection and analysis. JLG, FG, MN, and RR provided supervision and reviewed the manuscript.

Funding Open Access Funding provided by Universitat Autonoma de Barcelona. This research was supported by grant PID2022-139019OB-I00 (Plan General del Conocimiento, Ministerio de Ciencia, Innovación y Universidades, Gobierno de España). The research group Enginyeria de Bioprocessos i Biocatàlisi Aplicada ENG4BIO is recognized as 2021 SGR 00143 by Departament de Recerca i Universitats de la Generalitat de Catalunya. JLG is supported by The Novo Nordisk Foundation with grant number NNF22OC0078741 and Marie Skłodowska-Curie Actions (MSCA) Postdoctoral Fellowship 101105465. ADM is supported by the Industrial Doctorates Plan of the Department of Research and Universities of the Generalitat de Catalunya with grant number 2021DI009.

Data Availability No datasets were generated or analysed during the current study.

Declarations

Ethics Approval This article does not contain any studies with human participants or animals performed by any of the authors.

Competing interests The authors declare no competing interests.

References

Andreani, G., Sogari, G., Marti, A., Froldi, F., Dagevos, H., & Martini, D. (2023). Plant-based meat alternatives: Technological, nutritional, environmental, market, and social challenges and opportunities. *Nutrients, 15*(2), Article 452. https://doi.org/10.3390/nu15020452

Bartczak, M., Wierzchowski, K., & Pilarek, M. (2022). Mixing performance in a litre-scale rocking disposable bioreactor: DoE-based investigation of mixing time dependence on operational parameters. *Chemical Engineering Journal*. https://doi.org/10.1016/j.cej.2021.133288

Bellani, C. F., Ajeian, J., Duffy, L., Miotto, M., Groenewegen, L., & Connon, C. J. (2020). Scale-up technologies for the manufacture of adherent cells. *Frontiers in Nutrition*. https://doi.org/10.3389/fnut.2020.575146

Bielser, J. M., Wolf, M., Souquet, J., Broly, H., & Morbidelli, M. (2018). Perfusion mammalian cell culture for recombinant protein manufacturing – A critical review. *Biotechnology Advances, 36*(4), 1328–1340. https://doi.org/10.1016/j.biotechadv.2018.04.011

Bodiou, V., Moutsatsou, P., & Post, M. J. (2020). Microcarriers for upscaling cultured meat production. *Frontiers in Nutrition, 7*, 1–16. https://doi.org/10.3389/fnut.2020.00010

Cherry, R. S., & Papoutsakis, E. T. (1986). Hydrodynamic effects on cells in agitated tissue culture reactors. *Bioprocess Engineering, 1*, 29–41. https://doi.org/10.1007/BF00369462

Chu, T. J., & Peters, D. G. (2008). Serial analysis of the vascular endothelial transcriptome under static and shear stress conditions. *Physiological Genomics, 34*, 185–192. https://doi.org/10.1152/physiolgenomics.90201.2008.-We

Collignon, M. L., Delafosse, A., Calvo, S., Martin, C., Marc, A., Toye, D., & Olmos, E. (2016). Large-eddy simulations of microcarrier exposure to potentially damaging eddies inside mini-bioreactors. *Biochemical Engineering Journal, 108*, 30–43. https://doi.org/10.1016/j.bej.2015.10.020

Couto, P. S., Stibbs, D. J., Sanchez, B. C., Khalife, R., Panagopoulou, T. I., Barnes, B., et al. (2024). Generating suspension-adapted human mesenchymal stromal cells (S-hMSCs) for the scalable manufacture of extracellular vesicles. *Cytotherapy*. https://doi.org/10.1016/j.jcyt.2024.06.011

Croughan, M. S., Hamel, J.-F., & Wang, D. 1C. (1986). Hydrodynamic effects on animal cells grown in microcarrier cultures. *Biotechnology and Bioengineering, 29*, 130–141.

Croughan, M. S., Sayre, E. S., & Wang, D. 1C. (1989). Viscous reduction of turbulent damage in animal cell culture. *Biotechnology and Bioengineering, 33*, 862–872.

de Sá Silva, J., Mizukami, A., Gonzalez Gil, L. V., de Valeria Campos, J., B.G. Assis, O., Tadeu Covas, D., et al. (2019). Improving wave-induced motion bioreactor performance for human mesenchymal stromal cell expansion. *Process Biochemistry, 84*, 143–152. https://doi.org/10.1016/j.procbio.2019.06.004

Demirden, S. F., Kimiz-Gebologlu, I., & Oncel, S. S. (2024). Animal cell lines as expression platforms in viral vaccine production: A post Covid-19 perspective. *ACS Omega, 9*, 16904–16926. https://doi.org/10.1021/acsomega.3c10484

Dohmen, R. G. J., Hubalek, S., Melke, J., Messmer, T., Cantoni, F., Mei, A., et al. (2022). Muscle-derived fibro-adipogenic progenitor cells for production of cultured bovine adipose tissue. *Npj Science of Food*. https://doi.org/10.1038/s41538-021-00122-2

Eibl, R., Senn, Y., Gubser, G., Jossen, V., Van Den Bos, C., & Eibl, D. (2021). Cellular agriculture: Opportunities and challenges. *Annual Review of Food Science and Technology, 2021*, 51–73. https://doi.org/10.1146/annurev-food-063020

Fang, Z., Lyu, J., Li, J., Li, C., Zhang, Y., Guo, Y., et al. (2022). Application of bioreactor technology for cell culture-based viral vaccine production: Present status and future prospects. *Frontiers in Bioengineering and Biotechnology*. https://doi.org/10.3389/fbioe.2022.921755

Fish, K. D., Rubio, N. R., Stout, A. J., Yuen, J. S. K., & Kaplan, D. L. (2020). Prospects and challenges for cell-cultured fat as a novel food ingredient. *Trends in Food Science & Technology, 98*, 53–67. https://doi.org/10.1016/j.tifs.2020.02.005

Földes, A., Reider, H., Varga, A., Nagy, K. S., Perczel-Kovach, K., Kis-Petik, K., et al. (2021). Culturing and scaling up stem cells of dental pulp origin using microcarriers. *Polymers*. https://doi.org/10.3390/polym13223951

Fu, Y., Chen, Z., Li, C., & Liu, G. (2012). Establishment of a duck cell line susceptible to duck hepatitis virus type 1. *Journal of Virological Methods, 184*(1–2), 41–45. https://doi.org/10.1016/j.jviromet.2012.05.004

Genzel, Y., Dietzsch, C., Rapp, E., Schwarzer, J., & Reichl, U. (2010). MDCK and Vero cells for influenza virus vaccine production: A one-to-one comparison up to lab-scale bioreactor cultivation. *Applied Microbiology and Biotechnology, 88*(2), 461–475. https://doi.org/10.1007/s00253-010-2742-9

Goh, T. K. P., Zhang, Z. Y., Chen, A. K. L., Reuveny, S., Choolani, M., Chan, J. K. Y., & Oh, S. K. W. (2013). Microcarrier culture for efficient expansion and osteogenic differentiation of human fetal mesenchymal stem cells. *BioResearch Open Access, 2*(2), 84–97. https://doi.org/10.1089/biores.2013.0001

Grein, T. A., Loewe, D., Dieken, H., Weidner, T., Salzig, D., & Czermak, P. (2019). Aeration and shear stress are critical process parameters for the production of oncolytic measles virus. *Frontiers in Bioengineering and Biotechnology*, *7*(78). https://doi.org/10.3389/fbioe.2019.00078

Gutiérrez-Granados, S., Gòdia, F., & Cervera, L. (2018). Continuous manufacturing of viral particles. *Current Opinion in Chemical Engineering, 22*, 107–114. https://doi.org/10.1016/j.coche.2018.09.009

Hewitt, C. J., Lee, K., Nienow, A. W., Thomas, R. J., Smith, M., & Thomas, C. R. (2011). Expansion of human mesenchymal stem cells on microcarriers. *Biotechnology Letters, 33*(11), 2325–2335. https://doi.org/10.1007/s10529-011-0695-4

Hundt, B., Schänzler, A., & Reichl, U. (2005). Serum free cultivation of primary chicken embryo fibroblast in microcarrier systems for vaccine production. In F. Gòdia & M. Fussenegger (Eds.), *Animal Cell Technology meets Genomics*. Springer.

Jeske, R., Lewis, S., Tsai, A. C., Sanders, K., Liu, C., Yuan, X., & Li, Y. (2021). Agitation in a microcarrier-based spinner flask bioreactor modulates homeostasis of human mesenchymal stem cells. *Biochemical Engineering Journal*. https://doi.org/10.1016/j.bej.2021.107947

Jossen, V., Kaiser, S. C., Schirmaier, C., Herrmann, J., Tappe, A., Eibl, D., et al. (2014). Modification and qualification of a stirred

single-use bioreactor for the improved expansion of human mesenchymal stem cells at benchtop scale. *Pharmaceutical Bioprocessing, 2*(4), 311–322. https://doi.org/10.4155/pbp.14.29

Jossen, V., Schirmer, C., Mostafa Sindi, D., Eibl, R., Kraume, M., Pörtner, R., & Eibl, D. (2016). Theoretical and practical issues that are relevant when scaling up hMSC microcarrier production processes. *Stem Cells International*. https://doi.org/10.1155/2016/4760414

Julaey, M., Hosseini, M., & Amani, H. (2016). Stem cells culture bioreactor fluid flow, shear stress and microcarriers dispersion analysis using computational fluid dynamics. *J Appl Biotechnol Rep, 3*(2), 425–431.

Klatt, A., Wollschlaeger, J. O., Albrecht, F. B., Rühle, S., Holzwarth, L. B., Hrenn, H., et al. (2024). Dynamically cultured, differentiated bovine adipose-derived stem cell spheroids as building blocks for biofabricating cultured fat. *Nature Communications*. https://doi.org/10.1038/s41467-024-53486-w

Koh, B., Sulaiman, N., Fauzi, M. B., Law, J. X., Ng, M. H., Idrus, R. B. H., & Yazid, M. D. (2020). Three dimensional microcarrier system in mesenchymal stem cell culture: A systematic review. *Cell and Bioscience*, *10*(1). https://doi.org/10.1186/s13578-020-00438-8

Kulus, M., Jankowski, M., Kranc, W., Golkar Narenji, A., Farzaneh, M., Dzięgiel, P., et al. (2023). Bioreactors, scaffolds and microcarriers and in vitro meat production—Current obstacles and potential solutions. *Frontiers in Nutrition*. https://doi.org/10.3389/fnut.2023.1225233

Kunnen, S. J., Malas, T. B., Semeins, C. M., Bakker, A. D., & Peters, D. J. M. (2018). Comprehensive transcriptome analysis of fluid shear stress altered gene expression in renal epithelial cells. *Journal of Cellular Physiology, 233*(4), 3615–3628. https://doi.org/10.1002/jcp.26222

Lavado-García, J., Cervera, L., & Gòdia, F. (2020). An alternative perfusion approach for the intensification of virus-like particle production in HEK293 cultures. *Frontiers in Bioengineering and Biotechnology, 8*, 1–16. https://doi.org/10.3389/fbioe.2020.00617

Lawson, T., Kehoe, D. E., Schnitzler, A. C., Rapiejko, P. J., Der, K. A., Philbrick, K., et al. (2017). Process development for expansion of human mesenchymal stromal cells in a 50 L single-use stirred tank bioreactor. *Biochemical Engineering Journal, 120*, 49–62. https://doi.org/10.1016/j.bej.2016.11.020

Letcher, S. M., Rubio, N. R., Ashizawa, R. N., Saad, M. K., Rittenberg, M. L., Mccreary, A., et al. (2022). In vitro insect fat cultivation for cellular agriculture applications. *ACS Biomaterials Science & Engineering, 8*(9), 3785–3796. https://doi.org/10.1021/acsbiomaterials.2c00093

Lohr, V., Hädicke, O., Genzel, Y., Jordan, I., Büntemeyer, H., Klamt, S., & Reichl, U. (2014). The avian cell line AGE1.CR.pIX characterized by metabolic flux analysis. *BMC Biotechnology*, *14*(72). http://www.biomedcentral.com/1472-6750/14/72

López-Fernández, A., Garcia-Gragera, V., Lecina, M., & Vives, J. (2024). Identification of critical process parameters for expansion of clinical grade human Wharton's jelly-derived mesenchymal stromal cells in stirred-tank bioreactors. *Biotechnology Journal*. https://doi.org/10.1002/biot.202300381

Loubière, C., Delafosse, A., Guedon, E., Toye, D., Chevalot, I., & Olmos, E. (2019). Optimization of the impeller design for mesenchymal stem cell culture on microcarriers in bioreactors. *Chemical Engineering & Technology, 42*(8), 1702–1708. https://doi.org/10.1002/ceat.201900105

Madeline, B., Ribaud, S., Xenopoulos, A., Simler, J., Schwamborn, K., & Léon, A. (2015). Culturing a duck ES-derived cell line in single-use bioreactors: a rapid, efficient, and cost-effective vaccine manufacturing system based on suspension culture. *BioProcess International, 13*(Suppl 3), 26–33. (March Supplement).

Maillot, C., De Isla, N., Loubiere, C., Toye, D., & Olmos, E. (2022). Impact of microcarrier concentration on mesenchymal stem cell growth and death: Experiments and modeling. *Biotechnology and Bioengineering, 119*(12), 3537–3548. https://doi.org/10.1002/bit.28228

Maria, S., Bonneau, L., Fould, B., Ferry, G., Boutin, J. A., Cabanne, C., et al. (2023). Perfusion process for CHO cell producing monoclonal antibody: Comparison of methods to determine optimum cell specific perfusion rate. *Biochemical Engineering Journal*. https://doi.org/10.1016/j.bej.2022.108779

Monteil, D. T., Juvet, V., Paz, J., Moniatte, M., Baldi, L., Hacker, D. L., & Wurm, F. M. (2016). A comparison of orbitally-shaken and stirred-tank bioreactors: PH modulation and bioreactor type affect CHO cell growth and protein glycosylation. *Biotechnology Progress, 32*(5), 1174–1180. https://doi.org/10.1002/btpr.2328

Nelson, M. (2024). 30kL bioreactor run described as 'new standard' in biomanufacturing. https://www.bioprocessintl.com/facilities-capacity/30kl-bioreactor-run-described-as-new-standard-in-biomanufacturing. Accessed on 02/08/2024.

Nguyen, L. T., Bang, S., & Noh, I. (2019). Tissue regeneration of human mesenchymal stem cells on porous gelatin micro-carriers by long-term dynamic in vitro culture. *Tissue Engineering and Regenerative Medicine, 16*(1), 19–28. https://doi.org/10.1007/s13770-018-00174-8

Nikolay, A., Léon, A., Schwamborn, K., Genzel, Y., & Reichl, U. (2018). Process intensification of EB66® cell cultivations leads to high-yield yellow fever and Zika virus production. *Applied Microbiology and Biotechnology, 102*(20), 8725–8737. https://doi.org/10.1007/s00253-018-9275-z

Nogueira, D. E. S., Cabral, J. M. S., Rodrigues, C. A. V., MDPI AG. (2021). Single-use bioreactors for human pluripotent and adult stem cells: Towards regenerative medicine applications. *Bioengineering*. https://doi.org/10.3390/BIOENGINEERING8050068

OECD/FAO. (2025). OECD-FAO Agricultural Outlook 2025–2034. OECD Publishing, Paris / FAO. https://doi.org/10.1787/601276cd-en

Olmos, E., Loubiere, K., Martin, C., Delaplace, G., & Marc, A. (2015). Critical agitation for microcarrier suspension in orbital shaken bioreactors: Experimental study and dimensional analysis. *Chemical Engineering Science, 122*, 545–554. https://doi.org/10.1016/j.ces.2014.08.063

Panchalingam, K. M., Jung, S., Rosenberg, L., & Behie, L. A. (2015). Bioprocessing strategies for the large-scale production of human mesenchymal stem cells: A review Mesenchymal Stem/Stromal Cells - An update. *Stem Cell Research and Therapy*, *6*(1). https://doi.org/10.1186/s13287-015-0228-5

Papoutsakis, E. T. (1991). Fluid-mechanical damage of animal cells in bioreactors. *Trends in Biotechnology*. https://doi.org/10.1016/0167-7799(91)90145-8

Pasitka, L., Cohen, M., Ehrlich, A., Gildor, B., Reuveni, E., Ayyash, M., et al. (2023). Spontaneous immortalization of chicken fibroblasts generates stable, high-yield cell lines for serum-free production of cultured meat. *Nature Food, 4*(1), 35–50. https://doi.org/10.1038/s43016-022-00658-w

Pereira, PMdeCC., & Vicente, AFdosRB. (2013). Meat nutritional composition and nutritive role in the human diet. *Meat Science, 93*(3), 586–592. https://doi.org/10.1016/j.meatsci.2012.09.018

Pieralisi, I., Rodriguez, G., Micheletti, M., Paglianti, A., & Ducci, A. (2016). Microcarriers' suspension and flow dynamics in orbitally shaken bioreactors. *Chemical Engineering Research & Design, 108*, 198–209. https://doi.org/10.1016/j.cherd.2015.11.020

Pörtner, R. (2007). *Animal cell biotechnology: Methods and protocols* (2nd ed., vol. 24). Humana Press. https://doi.org/10.1007/978-1-59745-399-8

Qiao, C., Meng, F., Jang, I., Jo, H., Chen, Y. E., & Zhang, J. (2016). Deep transcriptomic profiling reveals the similarity between

endothelial cells cultured under static and oscillatory shear stress conditions. *Physiological Genomics, 48*, 660–666. https://doi.org/10.1152/physiolgenomics.00025.2016

Rafiq, Q. A., Brosnan, K. M., Coopman, K., Nienow, A. W., & Hewitt, C. J. (2013). Culture of human mesenchymal stem cells on microcarriers in a 5 L stirred-tank bioreactor. *Biotechnology Letters, 35*(8), 1233–1245. https://doi.org/10.1007/s10529-013-1211-9

Reddig, P. J., & Juliano, R. L. (2005). Clinging to life: cell to matrix adhesion and cell survival. *Cancer and Metastasis Reviews, 24*(3), 425–439. https://doi.org/10.1007/s10555-005-5134-3

Ritchie, H., Rosado, P., & Roser, M. (2023). Meat and dairy production. *OurWorldInData*. https://ourworldindata.org/meat-production. Accessed on 09/08/2024.

Rodrigues, M. E., Costa, A. R., Fernandes, P., Henriques, M., Cunnah, P., Melton, D. W., et al. (2013). Evaluation of macroporous and microporous carriers for CHO-K1 cell growth and monoclonal antibody production. *Journal of Microbiology and Biotechnology, 23*(9), 1308–1321. https://doi.org/10.4014/jmb.1304.04011

Sands, R., Meade, B., Seale, J. L., Jr., Robinson, S., & Seeger, R. (2023). *Scenarios of global food consumption: Implications for agriculture (Report No. ERR-323)*. U.S. Department of Agriculture, Economic Research Service. https://doi.org/10.32747/2023.8134356.ers

Schouwenberg, J. E., Van der Velden-de Groot, T., Blueml, G. (2010). Vaccine production utilizing the potential of microcarriers in disposable bioreactor. In T. Noll (Eds.), *Cells and culture*. ESACT Proceedings, vol 4. Springer. https://doi.org/10.1007/978-90-481-3419-9_138

Shaikh, S., Lee, E. J., Ahmad, K., Ahmad, S. S., Chun, H. J., Lim, J. H., et al. (2021). Cell types used for cultured meat production and the importance of myokines. *Foods*. https://doi.org/10.3390/foods10102318

Sharma, R., Harrison, S. T. L., & Tai, S. L. (2022). Advances in bioreactor systems for the production of biologicals in mammalian cells. *ChemBioEng Reviews, 9*(1), 42–62. https://doi.org/10.1002/cben.202100022

Shin, D. M., Kim, Y. J., Choi, Y. S., Kim, B. K., & Han, S. G. (2023). Duck fat: Physicochemical characteristics, health effects, and food utilizations. *LWT*. https://doi.org/10.1016/j.lwt.2023.115435

Sion, C., Loubière, C., Wlodarczyk-Biegun, M. K., Davoudi, N., Müller-Renno, C., Guedon, E., et al. (2020). Effects of microcarriers addition and mixing on WJ-MSC culture in bioreactors. *Biochemical Engineering Journal*. https://doi.org/10.1016/j.bej.2020.107521

Smetana, S., Mathys, A., Knoch, A., & Heinz, V. (2015). Meat alternatives: Life cycle assessment of most known meat substitutes. *International Journal of Life Cycle Assessment, 20*(9), 1254–1267. https://doi.org/10.1007/s11367-015-0931-6

Teale, M. A., Schneider, S., Eibl, D., van den Bos, C., Neubauer, P., & Eibl, R. (2023). Mesenchymal and induced pluripotent stem cell–based therapeutics: A comparison. *Applied Microbiology and Biotechnology*. https://doi.org/10.1007/s00253-023-12583-4

Thomassen, Y. E., Van Der Welle, J. E., Van Eikenhorst, G., Van Der Pol, L. A., & Bakker, W. A. M. (2012). Transfer of an adherent Vero cell culture method between two different rocking motion type bioreactors with respect to cell growth and metabolic rates. *Process Biochemistry, 47*(2), 288–296. https://doi.org/10.1016/j.procbio.2011.11.006

Timmins, N. E., Athanasas, S., Günther, M., Buntine, P., & Nielsen, L. K. (2011). Ultra-high-yield manufacture of red blood cells from hematopoietic stem cells. *Tissue Engineering, Part C: Methods, 17*(11), 1131–1137. https://doi.org/10.1089/ten.tec.2011.0207

Timmins, N. E., Kiel, M., Günther, M., Heazlewood, C., Doran, M. R., Brooke, G., & Atkinson, K. (2012). Closed system isolation and scalable expansion of human placental mesenchymal stem cells. *Biotechnology and Bioengineering, 109*(7), 1817–1826. https://doi.org/10.1002/bit.24425

Timmins, N. E., Palfreyman, E., Marturana, F., Dietmair, S., Luikenga, S., Lopez, G., et al. (2009). Clinical scale ex vivo manufacture of neutrophils from hematopoietic progenitor cells. *Biotechnology and Bioengineering, 104*(4), 832–840. https://doi.org/10.1002/bit.22433

Tsai, A. C., Liu, Y., Yuan, X., Chella, R., & Ma, T. (2017). Aggregation kinetics of human mesenchymal stem cells under wave motion. *Biotechnology Journal*. https://doi.org/10.1002/biot.201600448

Valsta, L. M., Tapanainen, H., & Männistö, S. (2005). Meat fats in nutrition. *Meat Science, 70*, 525–530. https://doi.org/10.1016/j.meatsci.2004.12.016

Wang, J. H. C., & Thampatty, B. P. (2006). An introductory review of cell mechanobiology. *Biomechanics and Modeling in Mechanobiology, 5*(1), 1–16. https://doi.org/10.1007/s10237-005-0012-z

Wierzchowski, K., Kuźmińska, A., & Pilarek, M. (2021). Intensification of chondrocytes proliferation by microcarriers and wave-induced mixing: Reynolds number influence on CP5 cells growth. *Chemical Engineering and Processing - Process Intensification*. https://doi.org/10.1016/j.cep.2021.108472

Wierzchowski, K., & Pilarek, M. (2024). Disposable rocking bioreactors: Recent applications and progressive perspectives. *Trends in Biotechnology, 42*(3), 261–264.

Xing, Z., Kenty, B. M., Li, Z. J., & Lee, S. S. (2009). Scale-up analysis for a CHO cell culture process in large-scale bioreactors. *Biotechnology and Bioengineering, 103*(4), 733–746. https://doi.org/10.1002/bit.22287

Yamamoto, K., Nogimori, Y., Imamura, H., & Ando, J. (2020). Shear stress activates mitochondrial oxidative phosphorylation by reducing plasma membrane cholesterol in vascular endothelial cells. *Proceedings of the National Academy of Sciences of the United States of America, 117*(52), 33660–33667. https://doi.org/10.1073/pnas.2014029117

Yang, J., Guertin, P., Jia, G., Lv, Z., Yang, H., & Ju, D. (2019). Large-scale microcarrier culture of HEK293T cells and Vero cells in single-use bioreactors. *AMB Express*. https://doi.org/10.1186/s13568-019-0794-5

Yun, S. H., Lee, D. Y., Lee, J., Mariano, E., Choi, Y., Park, J., et al. (2024). Current research, industrialization status, and future perspective of cultured meat. *Food Science of Animal Resources, 44*(2), 326–355. https://doi.org/10.5851/kosfa.2024.e13

Zagury, Y., Ianovici, I., Landau, S., Lavon, N., & Levenberg, S. (2022). Engineered marble-like bovine fat tissue for cultured meat. *Communications Biology*. https://doi.org/10.1038/s42003-022-03852-5

Zhan, C., Bidkhori, G., Schwarz, H., Malm, M., Mebrahtu, A., Field, R., et al. (2020). Low shear stress increases recombinant protein production and high shear stress increases apoptosis in human cells. *iScience*. https://doi.org/10.1016/j.isci.2020.101653

Zhang, U., Zhang, Y., Yan, C., & Yu, J. (1997). The culture of chicken embryo fibroblast cells on microcarriers to produce infectious bursal disease virus. *Applied Biochemistry and Biotechnology, 62*, 291–302.